Adaptive Reconfiguration of Protection Relays to Accommodate Distributed Generation Systems

by

Gehad Ouda

A THESIS SUBMITTED TO THE FACULTY OF GRADUATE STUDIES IN PARTIAL FULFILLMENT OF THE REQUIREMENTS FOR THE DEGREE OF

MASTER OF APPLIED SCIENCE

GRADUATE PROGRAM IN ELECTRICAL ENGINEERING AND COMPUTER SCIENCE

York University

Toronto, Ontario

April, 2022

Abstract

The rise in the installation of distributed generation systems (DGs) requires the reconfiguration of the protection system of the distribution network (DN) in place. Increased integration of DGs in the DN can cause incorrect tripping and false non-tripping of the overcurrent (OC) protection relays in the DN as well as increased possibilities of faults due to the aging infrastructure of DN. Incorrect tripping is also known as sympathetic tripping and false non-tripping is also known as blinding operation of an OC relay. As such, a reconfiguration of the adaptive protective OC relays is desired to mitigate the issues with increased DG penetration in the DN. A new algorithm is proposed in this thesis for adaptive, distributed protection relay reconfiguration for the DN with DGs. Through theoretical studies based on potential games and practical simulations, the OC relays' settings are reconfigured to adapt to the DN's changes in the system as a result of DG integration.

Acknowledgements

I would like to start by thanking my family for their long standing and continued support. The completion of this thesis would not have been possible without the continued guidance, support, patience, and understanding of my supervisor Dr. Pirathayini Srikantha. I would also like to extend my thanks to my fellow colleagues in the research group. Finally, a great thanks to my high school mathematics teacher, Mr. Deeb Dakak, whom without his inspiration, I would not be where I am today.

Table of Contents

List of Tables

List of Figures

Chapter 1

Introduction

Adaptive relaying involves the protection system automatically making changes to its current state to suit the changes in the conditions of the power grid taking place [1]. The concept of adaptive relaying has proven to be challenging in the context of overcurrent (OC) relay coordination with the presence of distributed generation systems (DGs) being incorporated into the conventional infrastructure of the power grid. The integration of DGs has adverse effects on OC protection among other protection systems in place [2]. Specifically, the OC relay coordination can be compromised due to changing fault current levels when multiple DGs are interconnected to the power grid. Further complications as a result of the compromised protection system renders the aging distribution networks (DNs) even more vulnerable. As such, these complications need to be addressed in an effort to stabilize the existing protection infrastructure in the DN.

1.1 Literature Review

Various works in the literature consider OC protection schemes in the presence of DGs. Such works can be roughly classified into six different classes: 1) Applying reduction of the DN into an equivalent circuit to compute relay settings for variable DGs [3, 4, 5] ; 2) Utilizing simplifying assumptions such as incorporating passive mechanical protective devices (e.g.

reclosers, fuses, and fault current limiters) and enforcing limiting threshold on DG capacities [6, 8], and [18]; 3) Computing optimal DG sizing and placement to accommodate weaknesses in the existing DN via constrained optimization problems [9]-[11], [19]; 4) Minimizing the relay operating time or the sum of the relay operating times in the DN via a constrained optimization problem [4], [20]-[22]; 5) Use of heuristic techniques to solve the optimization problems [9], [19]-[20]; and 6) Centralized approach to adaptive relaying via online schemes [7].

Proposals belonging to the first class do not scale well when the number of DGs integrated into the DN becomes large as this tends to increase the complexity of the originally reduced equivalent circuit [3]-[5].

For work belonging to the second class, coordinating protection relays by making limiting assumptions restricts the flexibility of accommodating diverse power entities into the DN. Additionally, mechanical devices such as fuses require maintenance personnel to be sent in order to replace them which is time consuming and costly unlike an OC relay that can instantly reset without the need of the same resources as replacing mechanical devices. Moreover, the use of a fault current limiter (FCL) as proposed in [18] becomes very costly in which more FCLs would be required for larger DNs.

Existing proposals belonging to the third category attempt to compute the optimal placement of DGs along with the generation capacities to accommodate the current configuration of the DN [9]-[11]. As the characteristics of the typically aging DN infrastructure dictate the integration of diverse power entities, this approach tends to significantly restrict the flexible integration of diverse power entities.

Proposals with respect to the fourth class use the traditional relay characteristic curves and their variations. According to [23], the relay tripping times are restricted to the shape of the characteristic curves. Hence the approach to discretize the relay settings. With respect to the fifth class, [9] implements a Genetic Algorithm (GA) to solve the optimization problem given the fault current levels and relay settings as constraints. [19] utilizes NLP optimization

to maximize DG penetration in the DN using Particle Swarm Optimization (PSO) to solve the optimization problem. The heuristic method used in [20] is the Gravitational Search Algorithm (GSA). The heuristic techniques applied by [9, 19], and [20] may result in producing local optima but not global optima. Using of a centralized approach as proposed in [7] from the sixth class though attractive can have considerable disadvantages. Single point of failure can occur which results in the maloperation of the centralized system.

1.2 Problem Statement and Thesis Objectives

The traditional DN was designed with a unidirectional current flow in mind. This in turn also means that the protection system of the traditional DN was also designed with the assumption of current flowing in one direction in the DN. This assumption has proven to be a major problem in today's DN as bidirectional current flow is present with the incorporation of DGs in the DN. This further complicates the operation of the protection system in which traditionally, a line would be tripped when a reverse current is detected by the protection relays in the DN.

Overcurrent protection is the commonly used form of distribution line protection against fault currents. In distribution networks, digital relays connected circuit breakers are providing protection to a distribution feeder though they are not the only protection devices used.

The installation of DG on an existing distribution network can have multiple effects on the protection of the grid. Looking at Fig. 1.1, when a fault occurs at F1, DG1 contributes the fault current which results in an increased current flowing through the fuse near F1. This increased current due to the contribution from DG1 may be above the fuse ampere rating which was likely sized and selected based on the condition of the line without DG1 being connected to it [1]. This undersizing applies to other mechanical protective devices as well indicating one of the important considerations when installing DGs in the grid.

Another effect of connecting DGs to the grid is the potential occurrence of the unintended

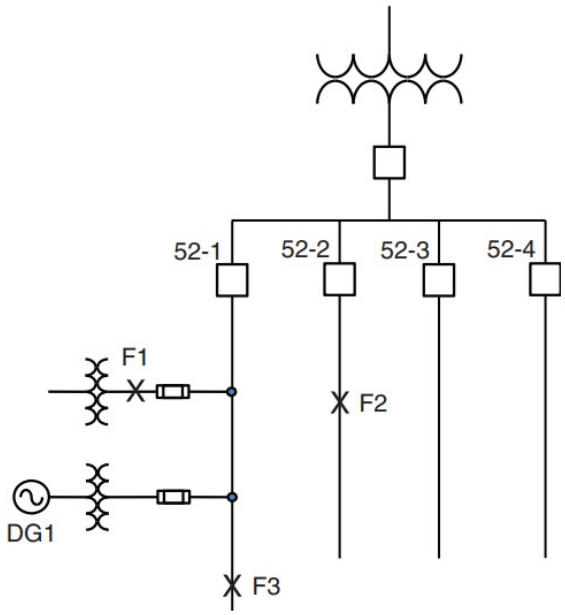

Figure 1.1: A radial distribution feeder with DG installed [1].

islanding phenomenon in the case of a microgrid [1]. When a fault occurs, the circuit breaker connecting main power grid and microgrid trips which results in an unplanned islanded operation of the microgrid. Such a disconnection results in an unsynchronized frequency and phase angle in between the two grids. The recloser attempts to reconnect the two grids after the circuit breaker has tripped. This reclosing results in a large phase difference in between the two grids. This phase difference can produce large inrush current transients that could damage the equipment, machinery, and even the DGs connected [1].

Summarizing what has been discussed thus far on the impact of DG on grid protection, false tripping also known as nuisance tripping of relays take place along with increased short-circuit current levels flowing in the grid. Bidirectional current flow in feeder occurs as part of the fault current contribution by the DG unlike the unidirectional flow with the conventional grid without the use of DGs. Finally, the unintended islanding of operation of a microgrid-main power grid connected network. The behavior of the fault current and the fault scenarios associated with the presence of DGs in the DN are discussed in the next chapter.

This thesis proposes a novel algorithm which that enables the decentralized reconfigu-

ration of protection relays that adapts to the changing conditions in the DN. Decentralized tuning of protection relays does not result in a single point of failure as opposed to central tuning. Consequently, self-healing of the DN is achieved. In other words, with decentralized tuning, the protection system adapts to the failure of the network. Such adaptation is based off of the cyber-physical capability of the power grid that allows for ubiquitous communication and computation by distribution grid elements [12]. As such, the main contributions of the thesis are summarized as follows:

1. An adaptive overcurrent relay reconfiguration algorithm that responds to different changes in DG capacities, fault, and load conditions in the DN is proposed.

2. Demonstration of the proposed algorithm preventing the sympathetic tripping and blinding operation of the OC relays in the presence of DGs operating in the DN.

3. Formulating a through a game theoretic approach from potential game thoery guaranteeing a convergence in finite-time to the Nash Equilibrium which translates into convergence to the optimal relay settings computed. The details of this convergence will be introduced and discussed in chapter 4.

4. Evaluation of the practical performance of the proposed decentralized algorithm on multiple DN feeders of different sizes.

5. Depiction of the algorithm not having a restriction on the size and location of DGs without compromising OC relay settings.

1.3 Thesis Outline

The remainder of this thesis is organized as follows. Chapter 2 presents the different fault scenarios that occur on DNs as a result of DGs complicating the normal response to the faults by the protection system followed by case studies demonstrating the same effects via numerical data. Chapter 3 outlines the fault current model and how short-circuit currents in

the presence of the DGs in the DN are computed using the DN bus impedance matrix followed by examples of the process. Chapter 4 builds the theory behind the decentralized algorithm and applies it to the 136-bus and 14-bus feeders of which the results are demonstrated as well. Finally, the conclusion and future directions are discussed in chapter 5 of this thesis.

Chapter 2

Fault Scenarios Affecting System Protection

The presence of DGs in a DN affects the fault current behaviour depending of the location of the fault as well as the location of the bus to which the DG is connected to. The consequences of the in-feed of the DGs into the DN on the protection system are discussed and are presented as five distinct fault scenarios. The thirty-three bus network is used in the explanation of each scenario [15].

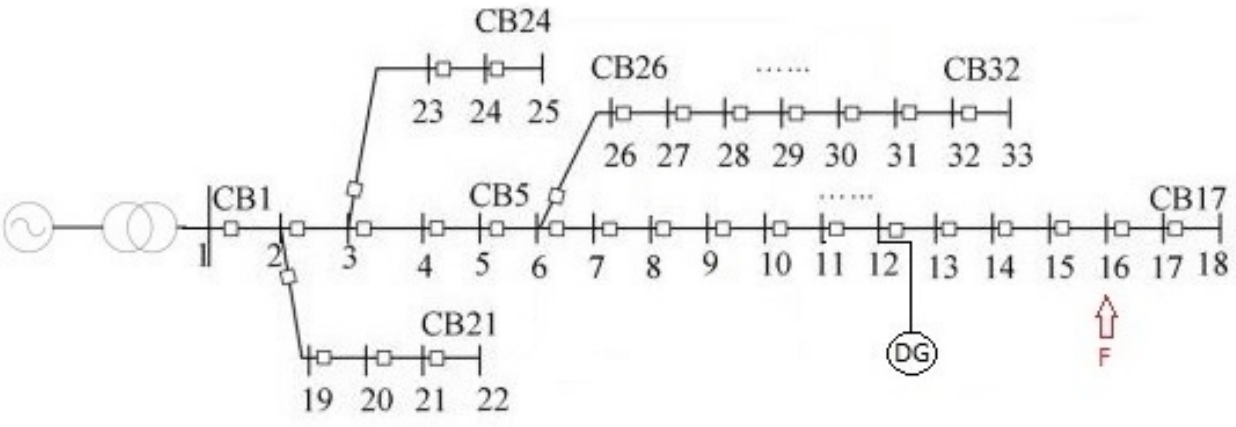

Figure 2.1: IEEE 33-bus feeder for scenarios 1 and 2.

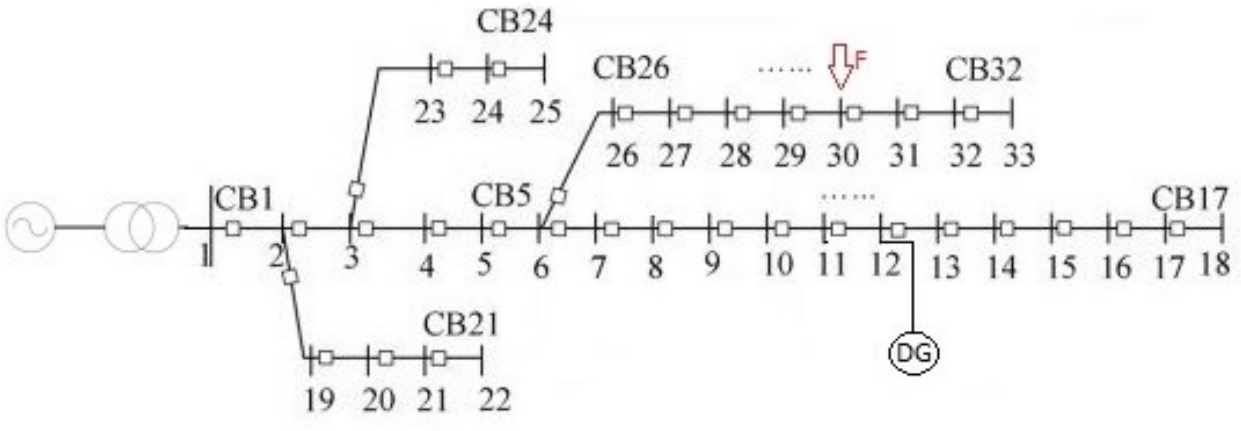

Figure 2.2: IEEE 33-bus feeder for scenario 3.

2.1 Decrease in upstream fault current

When a fault downstream the DG shown in Fig. 2.1 occurs, the short-circuit current upstream the DG decreases resulting in a potential false non-tripping of a relay that is located upstream the DG due to the short-circuit current seen by the relay being smaller in magnitude than its trip setting.

2.2 Increase in downstream fault current

In the event of a fault occurring downstream the DG in Fig. 2.1, the downstream short-circuit current increases as a result of the DG feeding the fault. If there is more than one relay that is located downstream the DG capable of tripping and isolating the fault, the increase in the downstream short-circuit current can result in the relay further away from the fault to trip resulting in a larger than necessary power outage.

2.3 Reverse current feeding from adjacent feeder

The occurrence of a fault on separate branch as depicted in Fig. 2.2, results in a reverse short-circuit current flowing from the adjacent branch to which a DG is connected. Again,

the DG is contributing to the fault. The reverse short-circuit current will falsely trip a relay if the magnitude of the reverse short-circuit is beyond the minimum relay setting at which it trips resulting in the unwanted loss of the adjacent branch. Also, if a relay on the same branch as the fault, is upstream the fault, and is protecting the faulted branch, it sees a higher magnitude short-circuit current resulting in the same issues discussed in the increase in downstream fault current scenario.

2.4 Multiple Faults

In the event of two separate faults occurring such as those shown in Fig. 1 and 2, the undesirable result of a larger outage as a result of the combination of the first three scenarios can occur. This can be generalized to situations in the DN where more than one fault occurs.

2.5 Multiple DGs

In the case where multiple DGs are present in a DN, the protection system may further be uncoordinated as a result of scenarios 1), 2), and 3) occurring all together depending on the location of the fault as well the location of the relays protecting the DN.

2.6 Case Studies with 33-Bus Feeder

2.6.1 Case study with the 33-Bus Feeder with one DG connected

To showcase the first two fault scenarios, the IEEE 33-bus feeder depicted in Fig. 2.1 is simulated in MATLAB without DGs for a bolted three-phase symmetrical fault at bus 16 with a substation capacity of 113 MVA. This simulation was implemented using the power systems toolbox from [14] through which the short-circuit currents were computed.
Table 2.1 demonstrates the short circuit currents in p.u. with no DGs in the DN. Table 2.2

Table 2.1: Short-circuit currents for a fault at bus 16.

From Bus	To Bus	Current Magnitude (p.u.)
1	2	0.1395
2	3	0.1395
3	4	0.1395
4	5	0.1395
5	6	0.1395
6	7	0.1395
7	8	0.1395
8	9	0.1395
9	10	0.1395
10	11	0.1395
11	12	0.1395
12	13	0.1395
13	14	0.1395
14	15	0.1395
15	16	0.1395

shows the short circuit currents in p.u. with a DG connected to bus 12 injecting at a capacity of 24 MVA. Comparing the two tables, it can be clearly seen that a decrease has occured in the short-circuit currents upstream the DG corresponding to first fault scenario and an increase in the short-circuit currents downstream the DG due to the DG contribution of the DG to the fault currents which corresponds to second fault scenario.

When the DG at bus 12 is injecting at an increased capacity of 34 MVA, it can be seen from the results in table 2.3 that a further increase in the short-circuit currents occurred downstream the DG again corresponding to the second fault scenario. Also, a further decrease in the short-circuit currents upstream the DG occurred again corresponding the first fault scenario.

The third fault scenario can be also be shown by simulating the IEEE 33 bus feeder illustrated in Fig. 2.2 for a fault at bus 30 with and without DG connected to the DN. The results are shown in tables 2.4 and 2.5. As it can be seen by comparing by comparing tables 2.4 and 2.5, a reverse short-circuit current is flowing from the DG at bus 12 corresponding to the third fault third scenario. In other words, there should be no fault currents flowing in

Table 2.2: Short-circuit currents for a fault at bus 16 with a DG at bus 12 injecting at a 24 MVA capacity.

From Bus	To Bus	Current Magnitude (p.u.)
1	2	0.0441
2	3	0.0441
3	4	0.0441
4	5	0.0441
5	6	0.0441
6	7	0.0441
7	8	0.0441
8	9	0.0441
9	10	0.0441
10	11	0.0441
11	12	0.0441
DG	12	0.2769
12	13	0.3050
13	14	0.3050
14	15	0.3050
15	16	0.3050

Table 2.3: Short-circuit currents for a fault at bus 16 with a DG at bus 12 injecting at a 34 MVA capacity.

From Bus	To Bus	Current Magnitude (p.u.)
1	2	0.0339
2	3	0.0339
3	4	0.0339
4	5	0.0339
5	6	0.0339
6	7	0.0339
7	8	0.0339
8	9	0.0339
9	10	0.0339
10	11	0.0339
11	12	0.0339
G	12	0.2981
12	13	0.3192
13	14	0.3192
14	15	0.3192
15	16	0.3192

Table 2.4: Short-circuit currents for a fault at bus 30.

From Bus	To Bus	Current Magnitude (p.u.)
1	2	0.2557
2	3	0.2557
3	4	0.2557
4	5	0.2557
5	6	0.2557
6	26	0.2557
26	27	0.2557
27	28	0.2557
28	29	0.2557
29	30	0.2557

the section of the DN that is between buses 6 and 18 for a fault at bus 30.

Table 2.5: Short-circuit currents for a fault at bus 30 with a DG at bus 12 injectiing at a 24 MVA capacity.

From Bus	To Bus	Current Magnitude (p.u.)
1	2	0.1968
2	3	0.1968
3	4	0.1968
4	5	0.1968
5	6	0.1968
6	26	0.3004
7	6	0.1044
8	7	0.1044
9	8	0.1044
10	9	0.1044
11	10	0.1044
DG	12	0.1044
12	11	0.1044
26	27	0.3004
27	28	0.3004
28	29	0.3004
29	30	0.3004

2.6.2 Case study with the 33-Bus Feeder with two DGs connected

Another case study is completed with two DGs injecting at a capacity of 24 MVA connected to the 33-bus feeder as depicted in Fig. 2.3. The resulting short circuit currents due to a fault at bus 16 are listed table 2.6. Based on the results from table 2.6, an increase in the short-circuit currents downstream the DG connected to bus 12 can be seen. Moreover, a decrease in the short-circuit currents uptream the DG connected to bus 12 is seen. Additionally, a reverse short-circuit current flowing from the adjacent branch as a result of the DG connected to bus 28 contributing to the fault current is observed. Clearly, this behavior of the short-circuit currents is a combination of all of the fault scenarios discussed.

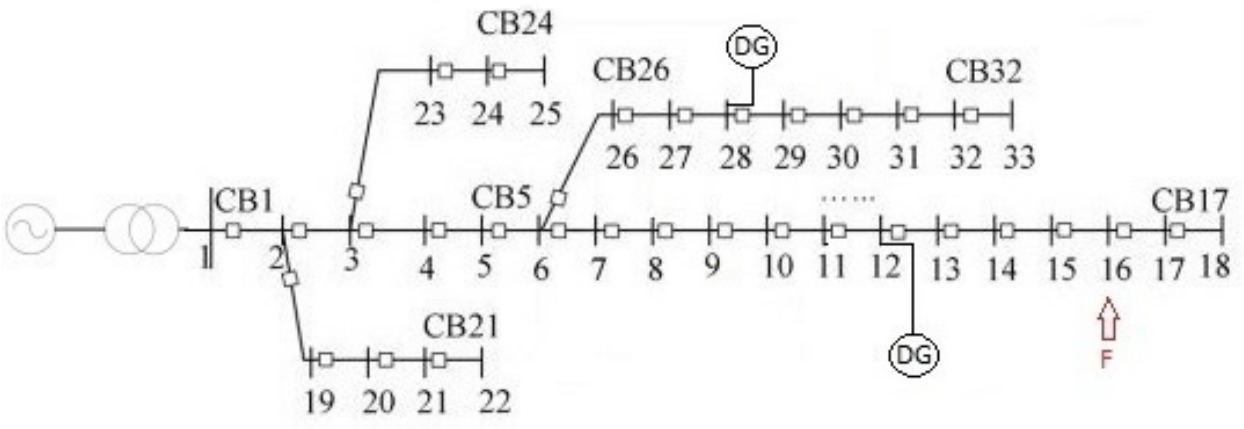

Figure 2.3: IEEE 33-bus feeder with two DGs connected.

2.7 Case Studies with 136-Bus Feeder

2.7.1 Case study with the 136-Bus Feeder with one DG connected

The different fault scenarios can also be observed in the Brazilian 136 bus DN [17]. The 136 bus DN is depicted in Fig. 2.4. The feeder is simulated for a fault at buses 28 and 68 without any DGs in the network. The resulting short-circuit currents as a result of a fault at buses 28 and 68 are shown Tables 2.7 and 2.8 respectively. Now suppose a DG connected

Table 2.6: Short-circuit currents for a fault at bus 12 with 2 DGs.

From Bus	To Bus	Current Magnitude (p.u.)
1	2	0.0273
2	3	0.0273
3	4	0.0273
4	5	0.0273
5	6	0.0273
6	7	0.0530
7	8	0.0530
8	9	0.0530
9	10	0.0530
10	11	0.0530
11	12	0.0530
DG	12	0.2701
12	13	0.3056
13	14	0.3056
14	15	0.3056
15	16	0.3056
DG	28	0.0265
28	27	0.0265
27	26	0.0265
26	6	0.0265

to bus 20 is injecting at a 24 MVA capacity, the resulting fault currents as a result of a fault occurring at buses 28 and 68 are listed in tables 2.9 and 2.10 respectively. Comparing tables 2.7 and 2.9, it can be seen that with the injection of the DG connected to bus 20 to the DN, a decrease in the short-circuit currents occurred upstream the DG between buses 1 and 20 corresponding to the fault scenario. Also, an increase in the short-circuit currents downstream the DG can be seen showcasing the second fault scenario. We can also see the effect of the third fault scenario by comparing tables 2.8 and 2.10. The DG connected to bus 20 is feeding the fault that has occurred at bus 68 demonstrating the reverse fault current as a result.

Table 2.7: Short-circuit currents for a fault at bus 28 on the 136-bus feeder.

From Bus	To Bus	Current Magnitude (p.u.)
1	18	0.6868
18	19	0.6868
19	20	0.6868
20	21	0.6868
21	23	0.6868
23	25	0.6868
25	26	0.6868
26	27	0.6868
27	28	0.6868

Table 2.8: Short-circuit currents for a fault at bus 68 on the 136-bus feeder.

From Bus	To Bus	Current Magnitude (p.u.)
1	64	0.5317
64	65	0.5317
65	66	0.5317
66	67	0.5317
67	68	0.5317

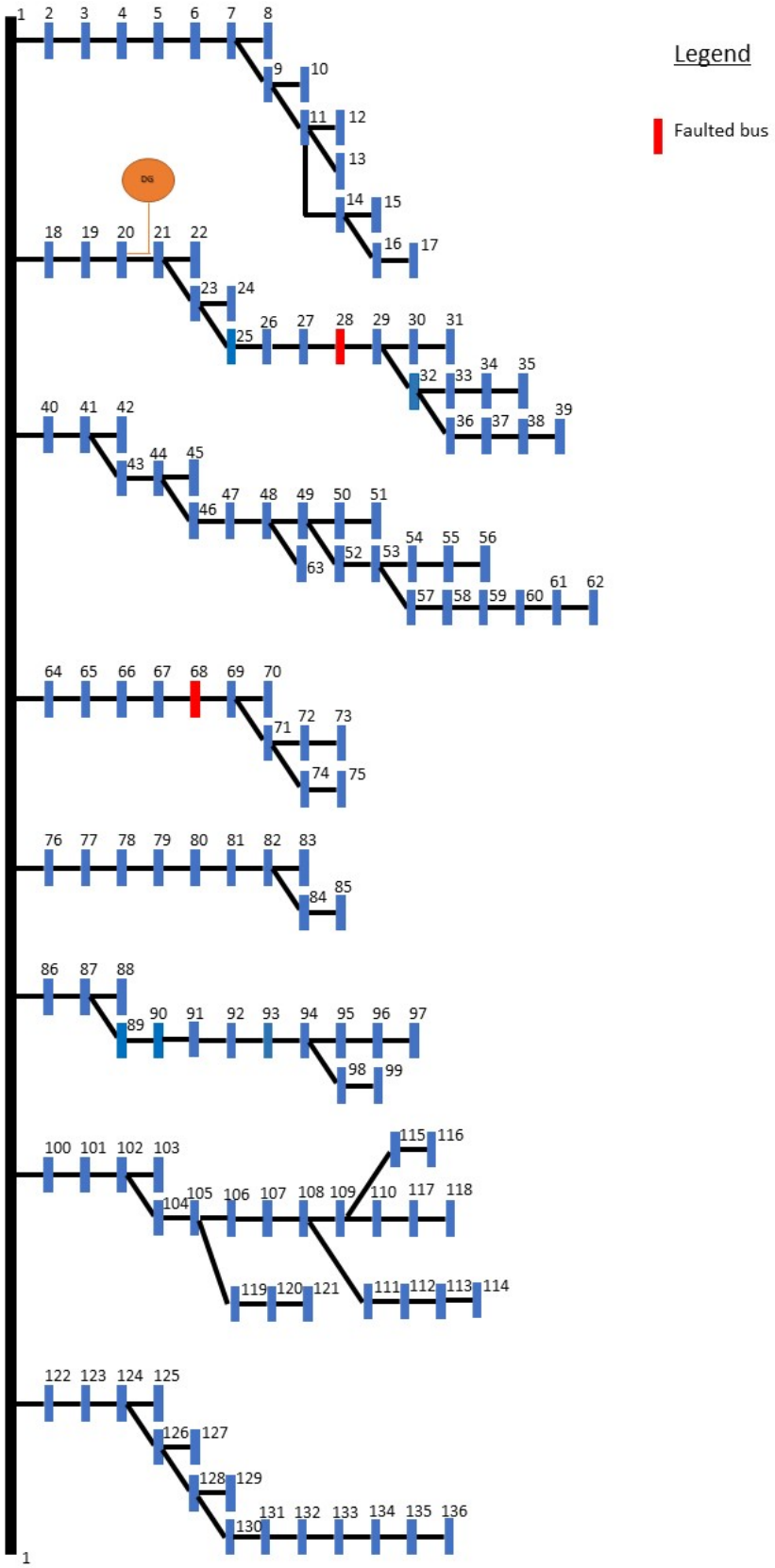

Figure 2.4: 136 bus feeder with one DG connected to bus 20.

Table 2.9: Short-circuit currents for a fault at bus 28 on the 136-bus feeder with DG at bus 20 injecting.

From Bus	To Bus	Current Magnitude (p.u.)
1	18	0.4664
18	19	0.4664
19	20	0.4664
DG	20	0.5835
20	21	1.035
21	23	1.035
23	25	1.035
25	26	1.035
26	27	1.035
27	28	1.035

Table 2.10: Short-circuit currents for a fault at bus 68 on the 136-bus feeder with DG at bus 20 injecting.

From Bus	To Bus	Current Magnitude (p.u.)
1	64	0.5352
64	65	0.5352
65	66	0.5352
66	67	0.5352
67	68	0.5352
DG	20	0.0517
20	19	0.0517
19	18	0.0517
18	1	0.0517

2.7.2 Case study with the 136-Bus Feeder with multiple DGs connected

The aim of this case study to verify and demonstrate that all of the fault scenarios occur. The 136-bus feeder shown in Fig. 2.5 is simulated in this case study. The short-circuit currents observed for a fault at buses 27, 67, and 91 without any of the DGs injecting into the grid are listed in tables 2.11, 2.12, and 2.13 respectively.

Table 2.11: Short-circuit currents for a fault at bus 27 on the 136-bus feeder.

From Bus	To Bus	Current Magnitude (p.u.)
1	18	0.7270
18	19	0.7270
19	20	0.7270
20	21	0.7270
21	23	0.7270
23	25	0.7270
25	26	0.7270
26	27	0.7270

Table 2.12: Short-circuit currents for a fault at bus 67 on the 136-bus feeder.

From Bus	To Bus	Current Magnitude (p.u.)
1	64	0.6906
64	65	0.6906
65	66	0.6906
66	67	0.6906

Table 2.13: Short-circuit currents for a fault at bus 91 on the 136-bus feeder.

From Bus	To Bus	Current Magnitude (p.u.)
1	86	0.7067
86	87	0.7067
87	89	0.7067
89	90	0.7067
90	91	0.7067

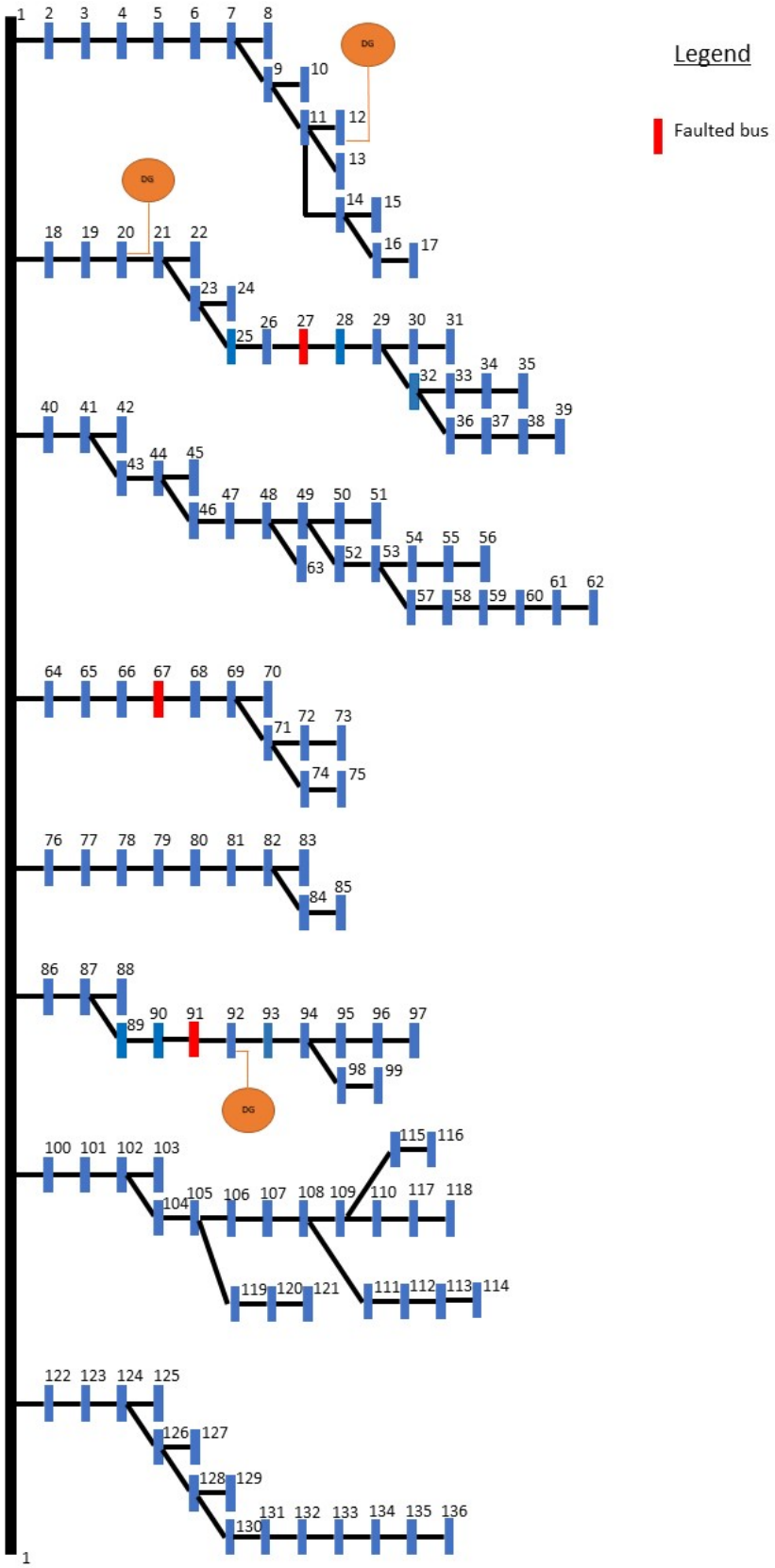

Figure 2.5: 136 bus feeder with multiple DGs connected.

Suppose the DG at bus 12 is injecting at a 24 MVA capacity, the corresponding short-circuit currents as a result of each fault are listed in tables 2.14, 2.15, and 2.16 respectively. It can be immediately seen from the mentioned tables that the DG at bus 12 is contributing to each of the three faults justifying the higher magnitudes in the branch currents closer to the fault locations. A reverse current as a result of the injecting DG can also be observed.

Table 2.14: Short-circuit currents for a fault at bus 27 on the 136-bus feeder with DG at bus 12 injecting at a 24 MVA capacity.

From Bus	To Bus	Current Magnitude (p.u.)
12	11	0.046228
11	9	0.046228
9	7	0.046228
7	6	0.046228
6	5	0.046228
5	4	0.046228
4	3	0.046228
3	2	0.046228
2	1	0.046228
1	18	0.73077
18	19	0.73077
19	20	0.73077
20	21	0.73077
21	23	0.73077
23	25	0.73077
25	26	0.73077
26	27	0.73077

Now, a second DG connected to bus 20 is injecting at a 28.3 MVA capacity along with the DG at bus 12. The resulting short-circuit currents for the three faults are illustrated in tables 2.17, 2.18, and 2.19. The fault at bus 27 is downstream the DG at bus 20 hence the added contribution to the fault at bus 27 in addition to the DG at bus 12 contributing. The fault currents between buses 18 to 20 have decreased for a fault at bus 27 as illustrated by table 2.17. These buses are upstream the DG connected to bus 20 and as such the behavior of the fault currents between buses 18 and 20 correspond to the first fault scenario. Increased fault currents were also observed for a fault at buses 67 and 91 as shown by tables 2.18, and

Table 2.15: Short-circuit currents for a fault at bus 67 on the 136-bus feeder with DG at bus 12 injecting at a 24 MVA capacity.

From Bus	To Bus	Current Magnitude (p.u.)
12	11	0.043923
11	9	0.043923
9	7	0.043923
7	6	0.043923
6	5	0.043923
5	4	0.043923
4	3	0.043923
3	2	0.043923
2	1	0.043923
1	64	0.69433
64	65	0.69433
65	66	0.69433
66	67	0.69433

Table 2.16: Short-circuit currents for a fault at bus 91 on the 136-bus feeder with DG at bus 12 injecting at a 24 MVA capacity.

From Bus	To Bus	Current Magnitude (p.u.)
12	11	0.044926
11	9	0.044926
9	7	0.044926
7	6	0.044926
6	5	0.044926
5	4	0.044926
4	3	0.044926
3	2	0.044926
2	1	0.044926
1	86	0.71019
86	87	0.71019
87	89	0.71019
89	90	0.71019
90	91	0.71019

2.19 respectively. This is again due to both DGs contributing the faults. Additionally, a reverse current as a result of each of the two injecting DGs from buses 12 and 20 is observed for the faults at buses 67 and 91 correponding to the third fault scenario.

Table 2.17: Short-circuit currents for a fault at bus 27 on the 136-bus feeder with DG at bus 20 injecting at a 28.3 MVA capacity.

From Bus	To Bus	Current Magnitude (p.u.)
12	11	0.030742
11	9	0.030742
9	7	0.030742
7	6	0.030742
6	5	0.030742
5	4	0.030742
4	3	0.030742
3	2	0.030742
2	1	0.030742
1	18	0.48597
18	19	0.48597
19	20	0.48597
20	21	1.172
21	23	1.172
23	25	1.172
25	26	1.172
26	27	1.172

Finally, the third DG that is connected to bus 92 is injecting in to the system at a capacity of 34 MVA capacity along with the other two DGs connected to buses 12 and 20. The resulting short-circuit currents for each of the three faults are listed tables 2.20, 2.21, and 2.22. It can be seen that there is a reverse current as a result of the DG at 92 contributing to each of the faults.

Through this case study, all of the fault scenarios were observed laying the groundwork for the upcoming chapters of this thesis.

Table 2.18: Short-circuit currents for a fault at bus 67 on the 136-bus feeder with DG at bus 20 injecting at a 28.3 MVA capacity.

From Bus	To Bus	Current Magnitude (p.u.)
12	11	0.040048
11	9	0.040048
9	7	0.040048
7	6	0.040048
6	5	0.040048
5	4	0.040048
4	3	0.040048
3	2	0.040048
2	1	0.040048
20	19	0.068274
19	18	0.068274
18	1	0.068274
1	64	0.70009
64	65	0.70009
65	66	0.70009
66	67	0.70009

Table 2.19: Short-circuit currents for a fault at bus 91 on the 136-bus feeder with DG at bus 20 injecting at a 28.3 MVA capacity.

From Bus	To Bus	Current Magnitude (p.u.)
12	11	0.040966
11	9	0.0040966
9	7	0.040966
7	6	0.040966
6	5	0.040966
5	4	0.040966
4	3	0.040966
3	2	0.040966
2	1	0.040966
20	19	0.069839
19	18	0.069839
18	1	0.069839
1	86	0.0.71614
86	87	0.71614
87	89	0.71614
89	90	0.71614
90	91	0.71614

Table 2.20: Short-circuit currents for a fault at bus 27 on the 136-bus feeder with DG at bus 92 injecting at a 34 MVA capacity.

From Bus	To Bus	Current Magnitude (p.u.)
12	11	0.029134
11	9	0.029134
9	7	0.029134
7	6	0.029134
6	5	0.029134
5	4	0.029134
4	3	0.029134
3	2	0.029134
2	1	0.029134
91	92	0.029798
91	90	0.029798
90	89	0.029798
89	87	0.029798
87	86	0.029798
86	1	0.029798
1	18	0.48597
18	19	0.48597
19	20	0.48597
20	21	1.1732
21	23	1.1732
23	25	1.1732
25	26	1.1732
26	27	1.1732

Table 2.21: Short-circuit currents for a fault at bus 67 on the 136-bus feeder with DG at bus 92 injecting at a 34 MVA capacity.

From Bus	To Bus	Current Magnitude (p.u.)
12	11	0.038071
11	9	0.038071
9	7	0.038071
7	6	0.038071
6	5	0.038071
5	4	0.038071
4	3	0.038071
3	2	0.038071
2	1	0.038071
20	19	0.064904
19	18	0.064904
18	1	0.064904
91	92	0.038939
91	90	0.038939
90	89	0.038939
89	87	0.038939
87	86	0.038939
86	1	0.038939
1	64	0.70295
64	65	0.70295
65	66	0.70295
66	67	0.70295

Table 2.22: Short-circuit currents for a fault at bus 91 on the 136-bus feeder with DG at bus 92 injecting at a 24 MVA capacity.

From Bus	To Bus	Current Magnitude (p.u.)
12	11	0.040966
11	9	0.0040966
9	7	0.040966
7	6	0.040966
6	5	0.040966
5	4	0.040966
4	3	0.040966
3	2	0.040966
2	1	0.040966
20	19	0.069839
19	18	0.069839
18	1	0.069839
1	86	0.0.71614
86	87	0.71614
87	89	0.71614
89	90	0.71614
90	91	0.71614
92	91	1.0897

Chapter 3

Fault Current Model

The superposition method is used to calculate the fault current. The fault state of a distribution network has two components, a normal component and an additive fault component. The normal component represents an unfaulted system while the additive fault component represents the impact of short circuit current. The additive fault component is calculated as a voltage vector and is then added to the node voltage to model the node voltage under fault condition [14]. The branch fault current is then calculated based on the node voltage under fault condition and the corresponding impedance of the branch where the (DG) is injecting.

The DG impedance is given by [9]:

$$Z_{DG} = x''_{dg} \frac{S_B}{S_{DG}} \tag{3.1}$$

where x''_{dg} is the subtransient reactance of the DG, S_B is the base MVA, and S_{DG} is DG capacity/power injected.

3.1 Bus Impedance Matrix Update

When a DG at a certain node k is injecting power onto a distribution feeder, it is the equivalent of a branch being added to the feeder between node k and ground. Due to this addition of the branch, the node impedance matrix has to be updated and is given by the formula as follows [9],[14]:

$$Z_{ij,new} = Z_{ij,old} - \frac{Z_{ik,old} Z_{kj,old}}{Z_{kk,old} + j Z_{DGk}} \tag{3.2}$$

where $Z_{ij,old}$, $Z_{ik,old}$, $Z_{kj,old}$ represent the mutual impedance prior to a change in DG injection between nodes i and j, nodes i and k, and nodes k and j, respectively; Z_{DGk} is the equivalent generator impedance associated with the DG; $Z_{ij,new}$ denotes the new mutual impedance associated with the new DG injection.

3.2 Branch Fault Current Computation

The additive fault component of the voltage vector when a bolted three-phase symmetrical fault occurs at node f in an N-bus network is computed as follows:

$$\Delta V_n = -Z_{new} I_f \tag{3.3}$$

$$\begin{bmatrix} \Delta V_1 \\ \vdots \\ \Delta V_f \\ \vdots \\ \Delta V_N \end{bmatrix} = \begin{bmatrix} Z_{11,new} & \dots & Z_{1f,new} & \dots & Z_{1N,new} \\ \vdots & \ddots & & & \\ Z_{f1,new} & & Z_{ff,new} & & Z_{fN,new} \\ \vdots & & & \ddots & \\ Z_{N1,new} & & Z_{Nf,new} & & Z_{NN,new} \end{bmatrix} \begin{bmatrix} 0 \\ \vdots \\ -I_f \\ \vdots \\ 0 \end{bmatrix} \tag{3.4}$$

where I_f is the fault current at bus f leaving the bus taken as negative current entering the bus. I_f is calculated using the following equation:

$$I_f = \frac{V_0}{Z_{ff,new}} \tag{3.5}$$

where V_0 is the prefault node voltage at node f which is equal to 1 p.u. in short circuit calculations and Z_{ff} is the self-impedance of node f. If the fault is unbolted, then the fault impedance is added to the denominator of equation (3.5). The node voltage of any node n in an N-bus network under a fault condition is thus given by:

$$V_n = V_0 + \Delta V_n \tag{3.6}$$

and the short-circuit current is calculated to as:

$$I_{ij} = \frac{V_i - V_j}{z_{ij}} \tag{3.7}$$

where z_{ij} is the line impedance of the branch connecting nodes i and j when DGs are installed. The short-circuit current in (3.7) can be expressed in terms of the mutual and line impedances by making the substitution from (3.4), (3.5), and (3.6) into (3.7). This yields (3.8) as follows:

$$I_{ij} = \frac{(Z_{jf,new} - Z_{if,new})\frac{1}{Z_{ff,new}}}{z_{ij}} \tag{3.8}$$

3.2.1 Example of the Fault Current Model

This section demonstrates an example of how short-circuit currents can be computed using equations (3.2) to (3.8) on the 33-bus feeder shown in Fig. 3.1. This section shall also serve as a prelude to section 4.2. Fig. 3.1 clearly shows that there is fault at bus 16 and a DG connected to bus 12 that is injecting. Suppose the branch fault current flowing from

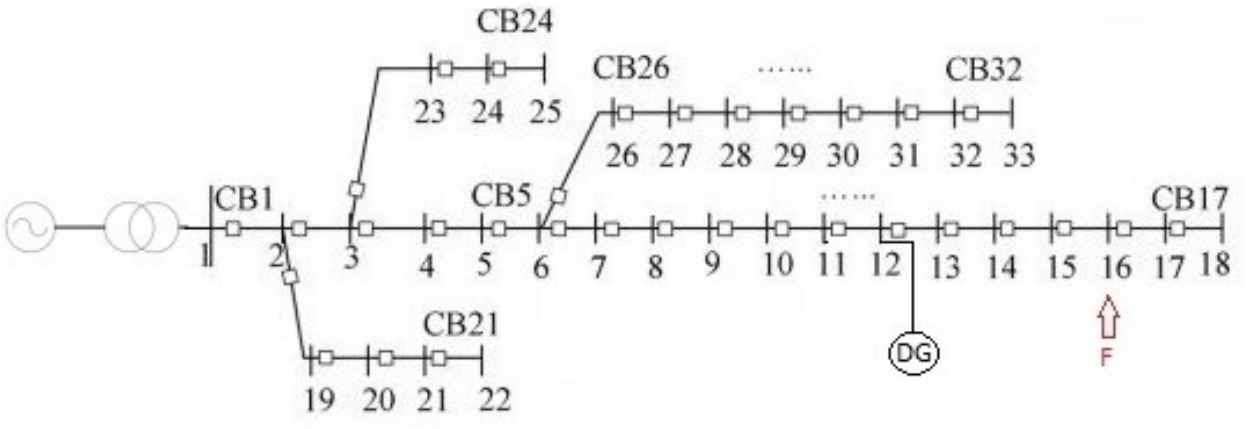

Figure 3.1: IEEE 33-bus feeder with DG at bus 12 and a fault at bus 16.

nodes 14 to 15 is needed. Using equation 3.8, it can be expressed as:

$$I_{14,15} = \frac{(Z_{15,16,new} - Z_{14,16,new})\frac{1}{Z_{16,16,new}}}{z_{14,15}} \tag{3.9}$$

In order to calculate the new mutual impedance and self-impedance terms in equation (3.9), equation (3.2) is utilized to update the mutual and self-impedance terms:

$$Z_{14,16,new} = Z_{14,16,old} - \frac{Z_{14,12,old}Z_{12,16,old}}{Z_{12,12,old} + jZ_{DG12}} \tag{3.10}$$

$$Z_{15,16,new} = Z_{15,16,old} - \frac{Z_{15,12,old}Z_{12,16,old}}{Z_{12,12,old} + jZ_{DG12}} \tag{3.11}$$

$$Z_{16,16,new} = Z_{16,16,old} - \frac{Z_{16,12,old}Z_{12,16,old}}{Z_{12,12,old} + jZ_{DG12}} \tag{3.12}$$

Then, equations (3.10) to (3.12) can be substituted into (3.9) to obtain the desired short-circuit current flowing from bus 14 to bus 15 as a result of a fault at bus 16 and DG injection from bus 12. Based on the calculation from this example, if the fault bus was to be labeled f and the DG bus was to be labeled k, then equations (3.10) to (3.12) can be re-written as:

$$Z_{14,f,new} = Z_{14,f,old} - \frac{Z_{14,k,old}Z_{k,f,old}}{Z_{k,k,old} + jZ_{DGk}} \tag{3.13}$$

$$Z_{15,f,new} = Z_{15,f,old} - \frac{Z_{15,k,old} Z_{k,f,old}}{Z_{k,k,old} + jZ_{DGk}} \tag{3.14}$$

$$Z_{f,f,new} = Z_{f,f,old} - \frac{Z_{f,k,old} Z_{k,f,old}}{Z_{k,k,old} + jZ_{DGk}} \tag{3.15}$$

Therefore, in order to compute the short-circuit current flowing from bus 14 to bus 15, the following terms are required:

$$\begin{array}{c|cc|c} Z_{k,f,old} & Z_{f.f,old} & & z_{14,15} \\ Z_{k,k,old} & Z_{14,f,old} & Z_{14,k,old} & \\ Z_{DGk} & Z_{15,f,old} & Z_{15,k,old} & \end{array}$$

This will be further generalized for all the short-circuit currents flowing in the DN in section 4.2.

3.2.2 Example of the Fault Current Model including bus impedance matrix computations

Consider the example 5-bus feeder shown in Fig. 3.2. Note that this structure of the feeder is selected for ease of demonstration. It is assumed that the bus impedance matrix

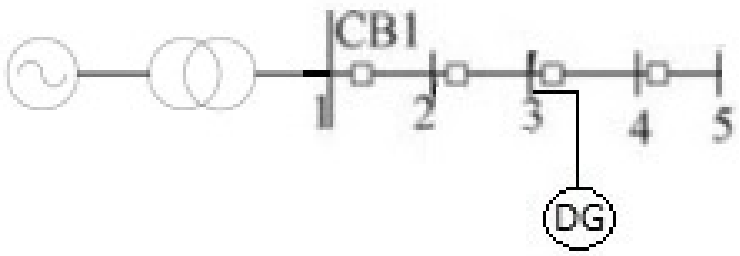

Figure 3.2: Example 5-bus feeder with a DG added.

of the 5-bus feeder is initially available without any DG injection. As such, the initial bus

impedance matrix of the example 5-bus feeder is as follows:

$$\begin{bmatrix} Z_{11} & Z_{12} & Z_{13} & Z_{14} & Z_{15} \\ Z_{21} & Z_{22} & Z_{23} & Z_{24} & Z_{25} \\ Z_{31} & Z_{32} & Z_{33} & Z_{34} & Z_{35} \\ Z_{41} & Z_{42} & Z_{43} & Z_{44} & Z_{45} \\ Z_{51} & Z_{52} & Z_{53} & Z_{54} & Z_{55} \end{bmatrix} \tag{3.16}$$

Fault at bus 2

If a fault occurs at bus 2, then the short-circuit currents flowing through the feeder are computed based on the bus impedance matrix shown by (3.16) and equation (3.8) are follows:

$$I_{12} = \frac{(Z_{22} - Z_{12})\frac{1}{Z_{22}}}{z_{12}} \tag{3.17}$$

$$I_{23} = \frac{(Z_{32} - Z_{22})\frac{1}{Z_{22}}}{z_{23}} \tag{3.18}$$

$$I_{34} = \frac{(Z_{42} - Z_{32})\frac{1}{Z_{22}}}{z_{34}} \tag{3.19}$$

$$I_{45} = \frac{(Z_{52} - Z_{42})\frac{1}{Z_{22}}}{z_{45}} \tag{3.20}$$

First DG Injection at bus 3

Suppose the DG connected to bus 3 starts injecting into the feeder, the DG impedance obtained from equation (3.1) is denoted by:

$$jZ_{DG3}^{(0)}$$

For a DG injection at bus 3, the corresponding bus impedance matrix components are updated using the following equation which is based off of equation (3.2):

$$Z_{ij}^{(0)} = Z_{ij} - \frac{Z_{i3}Z_{3j}}{Z_{33} + jx_{DG3}^{(0)}} \tag{3.21}$$

$$\begin{bmatrix} Z_{11}^{(0)} & Z_{12}^{(0)} & Z_{13}^{(0)} & Z_{14}^{(0)} & Z_{15}^{(0)} \\ Z_{21}^{(0)} & Z_{22}^{(0)} & Z_{23}^{(0)} & Z_{24}^{(0)} & Z_{25}^{(0)} \\ Z_{31}^{(0)} & Z_{32}^{(0)} & Z_{33}^{(0)} & Z_{34}^{(0)} & Z_{35}^{(0)} \\ Z_{41}^{(0)} & Z_{42}^{(0)} & Z_{43}^{(0)} & Z_{44}^{(0)} & Z_{45}^{(0)} \\ Z_{51}^{(0)} & Z_{52}^{(0)} & Z_{53}^{(0)} & Z_{54}^{(0)} & Z_{55}^{(0)} \end{bmatrix} \tag{3.22}$$

Fault at bus 2 after first DG injection

If a fault at bus 2 occurs after the DG injection. The short-circuit currents have to computed using the required updated bus impedance matrix components. This means that $Z_{12}^{(0)}$, $Z_{22}^{(0)}$, $Z_{32}^{(0)}$, $Z_{42}^{(0)}$, and $Z_{52}^{(0)}$ need to be computed.

$$Z_{12}^{(0)} = Z_{12} - \frac{Z_{13}Z_{32}}{Z_{33} + jx_{DG3}^{(0)}} \tag{3.23}$$

$$Z_{22}^{(0)} = Z_{22} - \frac{Z_{23}Z_{32}}{Z_{33} + jx_{DG3}^{(0)}} \tag{3.24}$$

$$Z_{32}^{(0)} = Z_{32} - \frac{Z_{33}Z_{32}}{Z_{33} + jx_{DG3}^{(0)}} \tag{3.25}$$

$$Z_{42}^{(0)} = Z_{42} - \frac{Z_{43}Z_{32}}{Z_{33} + jx_{DG3}^{(0)}} \tag{3.26}$$

$$Z_{52}^{(0)} = Z_{52} - \frac{Z_{53}Z_{32}}{Z_{33} + jx_{DG3}^{(0)}} \tag{3.27}$$

Then based on the updated bus impedance matrix components computed from equations (3.23) to (3.27) the short-circuit currents are computed are follows:

$$I_{12}^{(0)} = \frac{(Z_{22}^{(0)} - Z_{12}^{(0)})\frac{1}{Z_{22}^{(0)}}}{z_{12}} \tag{3.28}$$

$$I_{23}^{(0)} = \frac{(Z_{32}^{(0)} - Z_{22}^{(0)})\frac{1}{Z_{22}^{(0)}}}{z_{23}} \tag{3.29}$$

$$I_{34}^{(0)} = \frac{(Z_{42}^{(0)} - Z_{32}^{(0)})\frac{1}{Z_{22}^{(0)}}}{z_{34}} \tag{3.30}$$

$$I_{45}^{(0)} = \frac{(Z_{52}^{(0)} - Z_{42}^{(0)})\frac{1}{Z_{22}^{(0)}}}{z_{45}} \tag{3.31}$$

Second DG Injection at bus 3

Suppose the DG at bus 3 is now injecting a different capacity, the DG impedance obtained from equation (3.1) is denoted by:

$$jZ_{DG3}^{(1)}$$

For the new DG injection at bus 3, the corresponding bus impedance matrix components have to be re-updated using the following equation:

$$Z_{ij}^{(1)} = Z_{ij}^{(0)} - \frac{Z_{i3}^{(0)} Z_{3j}^{(0)}}{Z_{33}^{(0)} + jx_{DG3}^{(1)}} \tag{3.32}$$

$$\begin{bmatrix} Z_{11}^{(1)} & Z_{12}^{(1)} & Z_{13}^{(1)} & Z_{14}^{(1)} & Z_{15}^{(1)} \\ Z_{21}^{(1)} & Z_{22}^{(1)} & Z_{23}^{(1)} & Z_{24}^{(1)} & Z_{25}^{(1)} \\ Z_{31}^{(1)} & Z_{32}^{(1)} & Z_{33}^{(1)} & Z_{34}^{(1)} & Z_{35}^{(1)} \\ Z_{41}^{(1)} & Z_{42}^{(1)} & Z_{43}^{(1)} & Z_{44}^{(1)} & Z_{45}^{(1)} \\ Z_{51}^{(1)} & Z_{52}^{(1)} & Z_{53}^{(1)} & Z_{54}^{(1)} & Z_{55}^{(1)} \end{bmatrix}$$

If a fault at bus 2 occurs after the second DG injection, then as with the first the DG injection, the short-circuit currents have to computed using the re-updated bus impedance matrix components. This means that $Z_{12}^{(1)}$, $Z_{22}^{(1)}$, $Z_{32}^{(1)}$, $Z_{42}^{(1)}$, and $Z_{52}^{(1)}$ have to be computed.

$$Z_{12}^{(1)} = Z_{12}^{(0)} - \frac{Z_{13}^{(0)} Z_{32}^{(0)}}{Z_{33}^{(0)} + jx_{DG3}^{(1)}} \tag{3.33}$$

$$Z_{22}^{(1)} = Z_{22}^{(0)} - \frac{Z_{23}^{(0)} Z_{32}^{(0)}}{Z_{33}^{(0)} + jx_{DG3}^{(1)}} \tag{3.34}$$

$$Z_{32}^{(1)} = Z_{32}^{(0)} - \frac{Z_{33}^{(0)} Z_{32}^{(0)}}{Z_{33}^{(0)} + jx_{DG3}^{(1)}} \tag{3.35}$$

$$Z_{42}^{(1)} = Z_{42}^{(0)} - \frac{Z_{43}^{(0)} Z_{32}^{(0)}}{Z_{33}^{(0)} + jx_{DG3}^{(1)}} \tag{3.36}$$

$$Z_{52}^{(1)} = Z_{52}^{(0)} - \frac{Z_{53}^{(0)} Z_{32}^{(0)}}{Z_{33}^{(0)} + jx_{DG3}^{(1)}} \tag{3.37}$$

Thus, the short-circuit currents are given by:

$$I_{12}^{(1)} = \frac{(Z_{22}^{(1)} - Z_{12}^{(1)})\frac{1}{Z_{22}^{(1)}}}{z_{12}} \tag{3.38}$$

$$I_{23}^{(1)} = \frac{(Z_{32}^{(1)} - Z_{22}^{(1)})\frac{1}{Z_{22}^{(1)}}}{z_{23}} \tag{3.39}$$

$$I_{34}^{(1)} = \frac{(Z_{42}^{(1)} - Z_{32}^{(1)})\frac{1}{Z_{22}^{(1)}}}{z_{34}} \tag{3.40}$$

$$I_{45}^{(1)} = \frac{(Z_{52}^{(1)} - Z_{42}^{(1)})\frac{1}{Z_{22}^{(1)}}}{z_{45}} \tag{3.41}$$

A generalized form of the bus impedance matrix along with outline of the required components shall be discussed in further detail under section 4.2 of this thesis.

Chapter 4

Adaptive Decentralized Protection via Potential Game Approach

4.1 Assumptions

The following are the assumptions made in this thesis with respect to the underlying system model:

1. The DN has a radial topology;
2. The bus impedance matrix of the network prior to the integration of DGs is available;
3. Changes in generation capacity are accommodated by the algorithm one DG at a time;
4. Relays can communicate with one another and are capable of performing local computations;
5. Faults occurring in the DN are bolted three-phase symmetrical faults;
6. Fixed number of discrete relay settings are available for each protection relay installed in the DN; and
7. Probabilities of faults occurring at various locations in the DN are known.

The first assumption stems from the radial topology adopted by most practical DNs [12]. The second assumption is realistic as electric power utilities maintain information on the electrical characteristics of the DN [13]. The entire bus impedance matrix will not be shared with the participating relays. Only a small subset of this matrix will be needed for the proposed decentralized computation process outlined in section 4.2. As the simultaneous change in the generation capacity of DGs is highly unlikely, the third assumption is valid. The fourth assumption is supported by the cyber-physical vision for the modern smart grid [12]. The common mode of faults occurring in the DN is the bolted three-phase symmetrical faults - thereby supporting the fifth assumption [13]. Also, three-phase symmetrical faults can lead to the most damage as compared to other types of faults. The sixth assumption is practical as the tripping settings available in protection relays are discrete in nature and are typically common amongst these devices [14]. The final assumption is practical as electric power utilities (EPUs) maintain historical incident reports and are aware of vulnerable locations that can lead to fault conditions in the DN. This information can be readily utilized to compute these probabilities of faults [14].

4.2 Proposed Algorithm

This section which is split into two parts presents a detailed overview of the proposed decentralized algorithm. The first subsection presents the theoretical formulation based on game theory. The second subsection breaks down the computational steps and the algorithm implemented.

4.2.1 Game Theoretic Formulation

The basis of the decentralized algorithm is formulated using a game theoretic approach. The game $\mathcal{G}(\mathcal{P}, \mathcal{S}, J)$ is defined where $\mathcal{P}$ are the players, $\mathcal{S}$ is the set containing the strategies that can be selected by the players, and J is the cost function associated with each player

$i \in \mathcal{P}$. The players in this game are the OC relays in the DN and the strategies are the discrete relay settings available.

It was previously seen in this thesis that all of the scenarios discussed lead to some form of undesirable behavior by the relays as a result of the changing short-circuit currents when there is a change in DG injection into a DN. Namely, false tripping and false non-tripping of a relay and its consequences on a DN when faults occur. Based on the fault scenarios and their behavioral outcomes, the overall power outage is introduced in the following equation as the cost of tripping a relay which will be part of the cost function:

$$P^{a}_{outage}(S) \tag{4.1}$$

where S is the current set of relay trip settings selected by the relays and each component s_i takes values from $\mathcal{S}$. As previously discussed, tripping by a relay as a result of a fault observed does not ensure fault isolation. As such, the isolation needs to be accounted for in the formulation. Thus, the cost of isolation of a fault is defined using the log-barrier function:

$$\log(\mathbb{1}_a\{S\}), \text{ where } \mathbb{1}_a\{S\} = \begin{cases} +1, & \text{if fault } a \text{ is isolated} \\ 0, & \text{otherwise.} \end{cases} \tag{4.2}$$

It can be seen from equation (4.2) that in the event of fault not being isolated, a diversion to infinity will occur. Through this, the algorithm will specify that a fault must be isolated. This will be discussed in further detail shortly. In addition to the tripping and isolation requirements modeled by equations (4.1) and (4.2), each fault in the DN needs to be accounted for as it was observed from the fourth fault scenario that multiple faults can occur. This is done by incorporating the probability of each fault that can occur at each bus into the overall cost of the game defined by:

$$J(S) = \sum_{a \in \mathcal{F}} p_a \left[P^{a}_{outage}(S) - \log(\mathbb{1}_a\{S\}) \right] \tag{4.3}$$

where $\mathcal{F}$ is the set of various fault conditions possible in the DN and p_a is the probability of fault $a \in \mathcal{F}$ occurring in the DN. This probability can be computed by the EPU using historic trends of faults and environmental risk analysis (e.g. flora and fauna that can affect the integrity DN lines and components, age of infrastructure, etc.). The $\log(\mathbb{1}_a\{S\})$ term is a penalty term. Analyzing the cost function given by (4.3), should a relay incorrectly trip or incorrectly not trip, the aim of the $\log(\mathbb{1}_a\{S\})$ term is to penalize a relay for selecting a strategy that leads to the improper response to a fault. Specifically, should a fault not be isolated when a relay trips, the second term and hence the cost function diverges to infinity.

The players in game $\mathcal{G}$ are assumed to be selfish and aim to minimize their own individual cost irrespective of the strategy taken by the other players. This translates into the best-response strategy which results in the lowest cost for each player regardless of the strategy of others. In the context of this work, the best-response approach means that each relay will select a setting from S that will selfishly minimize its own individual cost. The best-response approach can be mathematically expressed as follows:

$$J(s_i^*, s_{-i}) \leq J(s_i, s_{-i}); \forall s_i \in \mathcal{S} \tag{4.4}$$

where s_i is the strategy selected by relay r_i and s_{-i} is the set of strategies selected by all other relays in the DN. It is worth noting that this game is an iterative game whereby a relay is randomly selected to change its strategy to satisfy the best-response approach given by equation (4.4) while the other relays do not change their strategies. There are multiple types of equilibrium that can be reached by the relays playing game $\mathcal{G}$ through the best-response approach. The convergence to the Nash equilibrium (NE) is considered in this work. At the NE, there is no incentive for any of the relays to unilaterally deviate from their current strategy. This means that each relay will have no regret in choosing their respective strategies. In practical terms, the guaranteed convergence to NE avoids the infinite switching to strategies by the relays without terminating at an optimal strategy. This infinite loop of strategy switches results in wasting large amounts of computational power along with the

algorithm failing. Thus, the importance of the NE. The NE is formally stated in equation as follows:

$$J(s_i^*, s_{-i}^*) \leq J(s_i, s_{-i}^*); \forall s_i \in S_i, \forall i \in P \tag{4.5}$$

where s_i^* and s_{-i}^* are the strategies that result in the NE. Now the question of whether the NE for game $\mathcal{G}$ exists or not must be addressed as not all games have a NE exist for them. In order to prove the existence of a NE, the concept of potential games is introduced. If a potential function Q can be defined such that it satisfies equation (4.6), then the NE equilibrium exists for game $\mathcal{G}$ [16].

$$\begin{aligned} &Q(t_i, s_{-i}) - Q(s_i, s_{-i}) > 0 \Leftrightarrow \\ &J_i(t_i, s_{-i}) - J_i(s_i, s_{-i}) > 0 \\ &\forall i \in P, \forall s_i \in \mathcal{S}, \forall t_i \in \mathcal{S}, \forall s_{-i} \in \mathcal{S} \end{aligned} \tag{4.6}$$

where J_i is the cost of individual players $i \in \mathcal{P}$. The cost function J defined in equation (4.3) for each player is a global cost function which can also be interpreted as the potential function Q. To further explain the conditions laid out by equation (4.6), the definition of a finite potential game is first stated. A finite potential game is a game with a finite strategy that admits a potential function [16]. A pure-strategy equilibrium can be achieved by the finite potential game within a finite number of iterations. This means that, according to [16], the game $\mathcal{G}$ will converge in finite time to the NE guaranteeing the existence of the NE.

4.2.2 Decentralized and Adaptive Computations

Given the DGs in a DN are non-dispatchable and inject at changing capacities at different time steps, it is necessary to compute the short-circuit currents seen by the relays protecting the DN in a decentralized manner to ensure the adaptive change in the relays' settings with the changes taking place in the DN.

If there is a change in DG capacity at bus k at time step s, any mutual and self-impedance from the bus impedance matrix in equation can be updated as follows.

$$Z_{i,j}^{(s)} = Z_{i,j}^{(s-1)} - \frac{Z_{i,k}^{(s-1)} Z_{k,j}^{(s-1)}}{Z_{k,k}^{(s-1)} + jZ_{dgk}^{(s)}} \tag{4.7}$$

Since the bus impedance matrix is symmetric, $Z_{k,j} = Z_{j,k}$
and thus equation (4.7) can be re-written as:

$$Z_{i,j}^{(s)} = Z_{ij}^{(s-1)} - \frac{Z_{i,k}^{(s-1)} Z_{j,k}^{(s-1)}}{Z_{k,k}^{(s-1)} + jZ_{dgk}^{(s)}} \tag{4.8}$$

The computation of a short-circuit current as a result of a fault at bus f seen by a relay located between buses a and b at time step s using the updated terms from the bus impedance matrix can be computed using equation (4.8) as follows:

$$I_{a,b}^{(s)} = \frac{(Z_{b,f}^{(s)} - Z_{a,f}^{(s)}) \frac{1}{Z_{f,f}^{(s)}}}{z_{a,b}} \tag{4.9}$$

Updating the full bus impedance matrix is computationally challenging and defeats the purpose of a decentralized approach. Based on (4.8), it can seen that a limited number of information exchanges are necessary for the computation of the changing DN parameters. As such, any short-circuit current, as a result of any faulted bus f, seen by a relay between any two consecutive buses a and b in an N bus network can be computed by only using the following terms from the bus impedance matrix:

$$\begin{bmatrix} & & Z_{1,k} & & \\ & & \vdots & & \\ Z_{a,1} & \dots & Z_{a,k} & \dots & Z_{a,N} \\ Z_{b,1} & \dots & Z_{b,k} & \dots & Z_{b,N} \\ & & \vdots & & \\ & & Z_{N,k} & & \end{bmatrix} \text{ and } diag(\mathbf{Z_{bus}}) \tag{4.10}$$

where $\mathbf{Z_{bus}}$ is the bus impedance matrix of the network. Therefore, it suffices to have the terms shown in (4.10) and update them as the system change rather than the whole of the bus impedance matrix. Algorithm 1 depicts a summary of the decentralized algorithm.

The algorithm is an offline algorithm triggered with a change in any of the DG injections in the observed DN. Based on this change, the relay settings are recomputed for different faults by switching their own strategies until convergence to the NE is achieved which also translates into successful tripping of the relay(s) that is closest to the fault(s) and the isolation of the fault(s). The cost function is a weighted average of the locally computed costs of the response of the OC relays to the faults in the DN. It is internal to the algorithm.

4.3 Results

The algorithm proposed in this paper is implemented in MATLAB and has been tested on the 136-bus system [17] which is illustrated in Fig. 4.1. Ninety eight relays are participating in the adaptive reconfiguration. These are located between each pair of buses from bus 1 to bus 99. These relays represent Players 1 to 98 in the order that they are listed. DGs are connected to buses 12, 20, and 92 with an initial generation capacity of 0 MVA. Faults occur at buses 27, 67, and 91 with probabilities of 20%, 35%, and 45% respectively. The available tripping settings that the relays can choose from are as follows: $[0.4, 0.5, 0.8, 1.0, 1.2, 1.4, 1.6, 2.0]$. This is computed using load flow analysis of the DN and various fault currents that can arise. The loads were adopted from the 136-bus system [17]. Three case studies are considered in the simulations: 1) DG at bus 12 is injecting at a 24 MVA capacity; 2) DG at bus 20 is injecting at 28.3 MVA capacity; and 3) DG at bus 91 is injecting at a 34 MVA capacity. The evolution of the cost in the system for these three case studies is illustrated in Fig. 4.2, Fig. 4.3, and Fig. 4.4.

In the first case study, relays (1-18), (18-19), (19-20), (20-21), (21-23), (23-25), (25-26), and (26-27) are capable of isolating the fault occurring at bus 27. Relay (26-27) is the one

Algorithm 1 Summary of Decentralized Algorithm

Initialization:

- Select a specified number of relays in the DN.
- Randomly assign a trip setting from S for each relay.

Algorithm:

- **For** $m = 1$: Number of DG Capacity Changes
    1. With a change in DG capacity occurring, update the terms from the bus impedance matrix from equation (4.10) with respect to each relay specified in the initialization using equation (3.2).
    2. Compute the short-circuit current seen by each relay by evaluating equation (3.8) using the updated bus impedance matrix computed in step 1).
        - **For**
    3. Select one relay at random.
    4. The relay selects another strategy from S to potentially switch to.
    5. Compute the cost as a result of this potential strategy switch. This is based on the response of the relays to the change in short-circuit currents computed in step 2 as a result of the change in DG capacity from step 1.
    6. Select a second relay at random that is on the same branch as the first relay from step 3.
    7. Switch ON the first relay by assigning it the lowest setting from S and switch OFF the second relay by assigning it the highest setting from S. Compute cost as a result.
    8. Switch OFF the first relay and switch ON the second relay using the same method as step 7 and compute the cost as a result.
    9. Compare the costs computed in steps 5,7, and 8 and select the potential strategy switch that resulted in the lower of the three costs.
    10. Compute the overall cost using equation (4.3).
    11. If a reduction in the overall cost seen by the relay is achieved, the relay(s) switches to the new strategy from step 9.
    12. Repeat steps 3 to 11 until convergence to the minimum overall cost is achieved for the fault condition.
        - **endFor**
- **endFor**

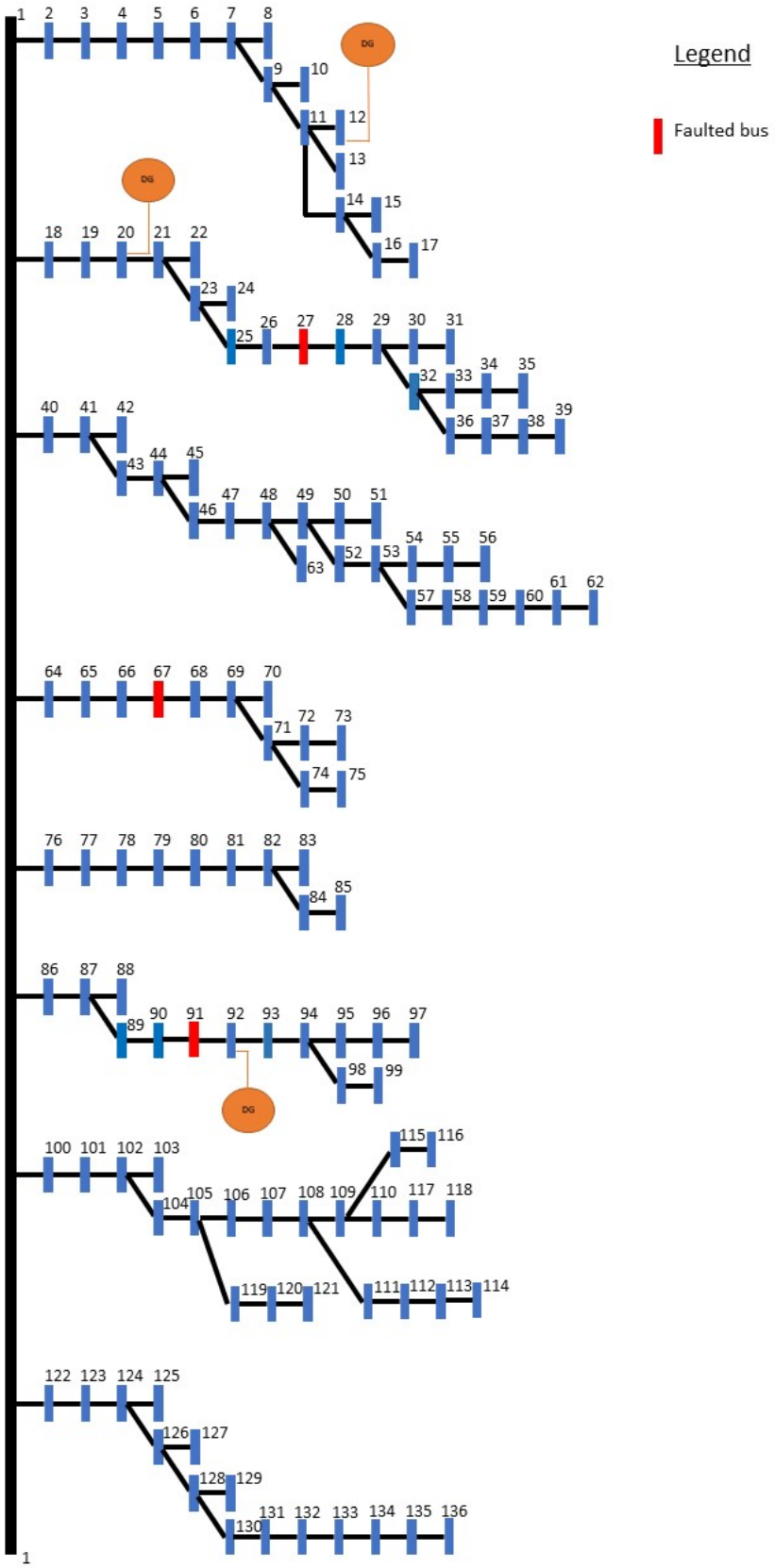

Figure 4.1: 136-bus system.

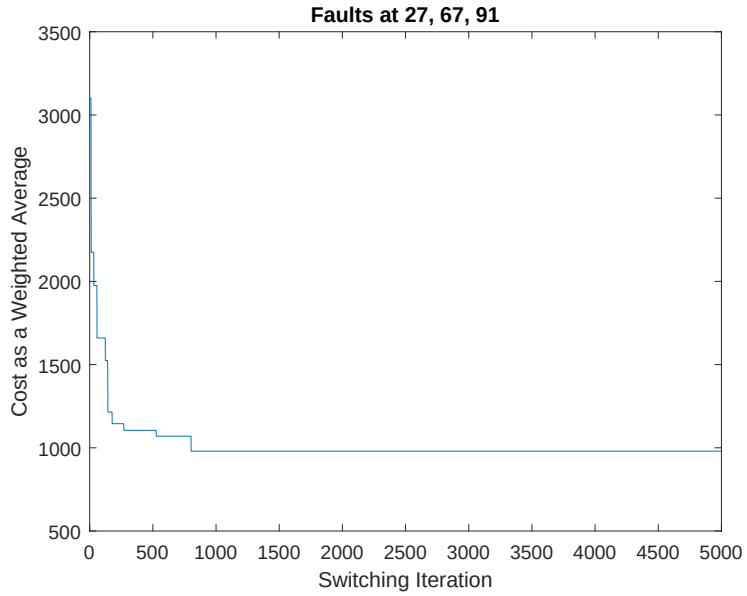

Figure 4.2: Case study 1. Evolution of players' strategies.

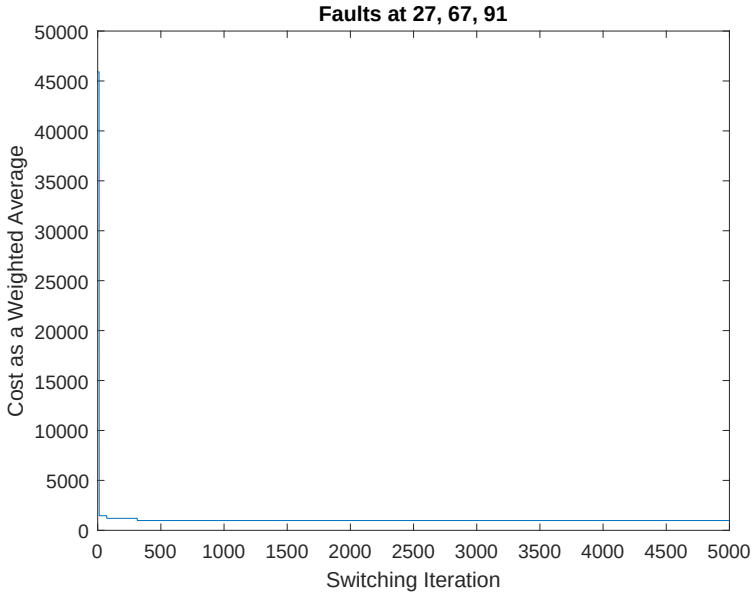

Figure 4.3: Case study 2. Evolution of players' strategies.

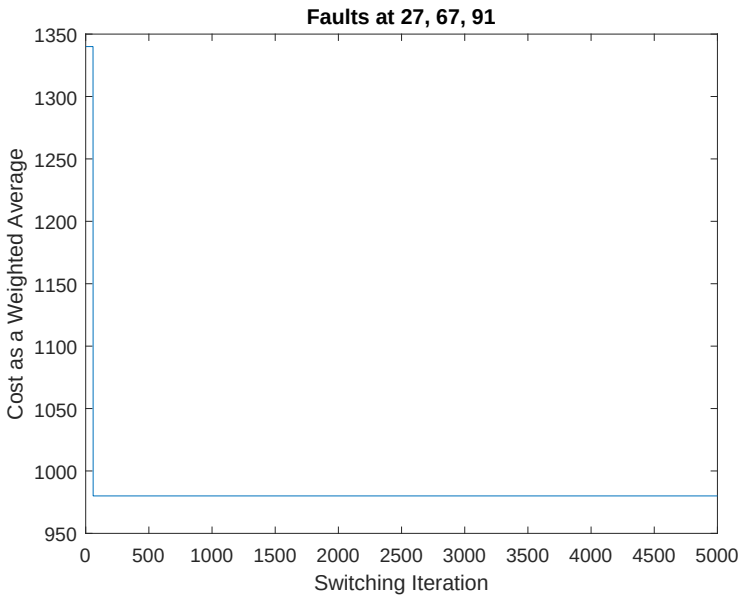

Figure 4.4: Case study 3. Evolution of players' strategies.

that is closest to the faulted bus 27 and results in the lowest outage when it trips as compared to relays (1-18), (18-19), (19-20), (20-21), (21-23), (23-25), and (25-26). As expected, relay (26-27) will trip for a fault at bus 27 as evident in Table 4.1 (i.e. relay (26-27) has a setting of 0.4 p.u. which is lower than 0.73077 p.u.). For a fault occurring at bus 67, relays (1-64), (64-65), (65-66), and (66-67) are capable of isolating the fault. Relay (66-67) is the one that is closest to the faulted bus 67 and results in the lowest outage when it trips as compared to (1-64), (64-65), and (65-66). Effectively, relay (66-67) trips for a fault at bus 67 as shown in TABLE 4.1 (i.e. relay (66-67) has a setting of 0.4 p.u. which is lower than 0.69433 p.u.). Relays (1-86), (86-87), (87-89), (89-90), and (90-91) are capable of isolating the fault occurring at bus 91. Relay (90-91) is the one that is closest to the faulted bus 91 and results in the smallest outage when it trips as compared to (1-86), (86-87), (87-89), and (89-90). Thus, relay (90-91) trips for a fault at bus 91 as it can be seen from the settings in TABLE 4.1 (i.e. relay (90-91) has a setting of 0.4 p.u. which is lower than 0.71019 p.u.). Relays (1-2), (2-3), (3-4), (4-5), (5-6), (6-7), (7-9), (9-11), and (11-12) see a reverse fault current for a fault at buses 27, 67, and 91 as a result of the DG at bus 12 which corresponds to Scenario 3. None of the relays seeing a reverse fault current trip avoiding unnecessary outage

and tripping. In Fig. 4.2, the evolution of the global cost as every player makes a strategy revision is presented. It is clear that the system converges to the equilibrium in finite time as expected.

In the second case study, the fault currents seen by relays (20-21), (21-23), (23-25), (25-26), and (26-27) for a fault at bus 27 are increased. The fault at bus 27 is downstream to the DG at bus 20 corresponds to fault Scenario 2. The fault current seen by relays (1-18), (18-19), and (19-20) decreases when the DG starts injecting into the grid (i.e. Scenario 1). Also, the relays see a noticeable reverse fault current for a fault at buses 67 and 91 which pertains to Scenario 3. Again, relay (26-27) which is closest to the fault at bus 27 will result in the lowest outage when it trips. Relays (1-86), (86-87), (87-89), (89-90), and (90-91) observe increased fault currents for the fault at bus 91 due to DGs at buses 12 and 20. Despite this change in the fault current levels, relay (90-91) will trip and isolate these faults according to Table 4.2. Relays (1-64), (64-65), (65-66), and (66-67) observe an increase in fault current levels for a fault at bus 67. Tripping and isolating of the fault at bus 67 is retained by relay (66-67) despite the increase in the fault current magnitude. A reverse fault current is again observed by relays (1-2), (2-3), (3-4), (4-5), (5-6), (6-7), (7-9), (9-11), and (11-12) for a fault at buses 27, 67, and 91 but none of these relays trip as demonstrated in Table 4.2. Once again, it can be observed from Fig. 4.3 that the cost evolution as the relays revise local strategies monotonically decreases and reaches an equilibrium in finite time.

In the third case study, the fault currents observed by relays (20-21), (21-23), (23-25), (25-26), and (26-27) for a fault at bus 27 is further increased due to the contribution of the DG at bus 92 to the fault at bus 27. Also, the fault current observed by relays (1-18), (18-19), and (19-20) for a fault at bus 27 has increased as well. Again, relays (1-18), (18-19), and (19-20) observe a reverse fault current for a fault at buses 67 and 91. Relays (1-64), (64-65), (65-66), and (66-67) observe an increase in fault current levels for a fault at bus 67 as a result of the now contributing DG at bus 92 to the fault. Relays (1-86), (86-87), (87-89), (89-90), and (90-91) observe a reverse fault current for a fault at buses 27 and 67. This is a

Table 4.1: Case study 1.

Relay	I_F (bus 27)	I_F (bus 67)	I_F (bus 91)	$TripSetting$
1 - 2	0.046228	0.043923	0.044926	0.8
2 - 3	0.046228	0.043923	0.044926	2
3 - 4	0.046228	0.043923	0.044926	1.4
4 - 5	0.046228	0.043923	0.044926	1.4
5 - 6	0.046228	0.043923	0.044926	1
6 - 7	0.046228	0.043923	0.044926	0.5
7 - 8	0	0	0	0.8
7 - 9	0.046228	0.043923	0.044926	2
9 - 10	0	0	0	1
9 - 11	0.046228	0.043923	0.044926	1.2
11 - 12	0.046228	0.043923	0.044926	1.4
11 - 13	0	0	0	0.8
11 - 14	0	0	0	1.4
14 - 15	0	0	0	1
14 - 16	0	0	0	0.4
16 - 17	0	0	0	0.8
1 - 18	0.73077	0	0	1
18 - 19	0.73077	0	0	0.8
19 - 20	0.73077	0	0	1
20 - 21	0.73077	0	0	2
21 - 22	0	0	0	1.2
21 - 23	0.73077	0	0	2
23 - 24	0	0	0	1.2
23 - 25	0.73077	0	0	0.8
25 - 26	0.73077	0	0	1.2
26 - 27	0.73077	0	0	0.4
27 - 28	0	0	0	1.4
28 - 29	0	0	0	0.8
29 - 30	0	0	0	1.6
30 - 31	0	0	0	1.4
29 - 32	0	0	0	0.8
32 - 33	0	0	0	1.6
33 - 34	0	0	0	1.6
34 - 35	0	0	0	2
32 - 36	0	0	0	0.4
36 - 37	0	0	0	0.5
37 - 38	0	0	0	0.5
36 - 39	0	0	0	2
1 - 40	0	0	0	1.2
40 - 41	0	0	0	2
41 - 42	0	0	0	1.6
41 - 43	0	0	0	2
43 - 44	0	0	0	1.6
44 - 45	0	0	0	1.2
44 - 46	0	0	0	0.8
46 - 47	0	0	0	0.4
47 - 48	0	0	0	0.4
48 - 49	0	0	0	1.4
49 - 50	0	0	0	1.2
50 - 51	0	0	0	0.5
49 - 52	0	0	0	0.4
52 - 53	0	0	0	0.8
53 - 54	0	0	0	0.8
54 - 55	0	0	0	0.8
55 - 56	0	0	0	1.2
53 - 57	0	0	0	2
57 - 58	0	0	0	1.6
58 - 59	0	0	0	2
59 - 60	0	0	0	1.2
60 - 61	0	0	0	0.4
61 - 62	0	0	0	0.4
48 - 63	0	0	0	1.4
1 - 64	0	0.69433	0	1.6
64 - 65	0	0.69433	0	1.4
65 - 66	0	0.69433	0	1.6
66 - 67	0	0.69433	0	0.4
67 - 68	0	0	0	1.4
68 - 69	0	0	0	1
69 - 70	0	0	0	2
69 - 71	0	0	0	2
71 - 72	0	0	0	1
72 - 73	0	0	0	0.8
71 - 74	0	0	0	2
74 - 75	0	0	0	1.4
1 - 76	0	0	0	1
76 - 77	0	0	0	1.6
77 - 78	0	0	0	1.2
78 - 79	0	0	0	0.4
79 - 80	0	0	0	1
80 - 81	0	0	0	0.4
81 - 82	0	0	0	1.2
82 - 83	0	0	0	1
82 - 84	0	0	0	2
84 - 85	0	0	0	1.6
1 - 86	0	0	0.71019	1.4
86 - 87	0	0	0.71019	1.6
87 - 88	0	0	0	1.2
87 - 89	0	0	0.71019	1.4
89 - 90	0	0	0.71019	0.8
90 - 91	0	0	0.71019	0.4
91 - 92	0	0	0	0.8
92 - 93	0	0	0	0.8
93 - 94	0	0	0	1
94 - 95	0	0	0	0.8
95 - 96	0	0	0	0.4
96 - 97	0	0	0	0.4
94 - 98	0	0	0	1.2
98 - 99	0	0	0	1.4

Table 4.2: Case study 2.

Relay	I_F (bus 27)	I_F (bus 67)	I_F (bus 91)	$TripSetting$
1 - 2	0.030742	0.040048	0.040966	1.4
2 - 3	0.030742	0.040048	0.040966	0.4
3 - 4	0.030742	0.040048	0.040966	0.5
4 - 5	0.030742	0.040048	0.040966	1.4
5 - 6	0.030742	0.040048	0.040966	0.8
6 - 7	0.030742	0.040048	0.040966	1
7 - 8	0	0	0	1
7 - 9	0.030742	0.040048	0.040966	1.2
9 - 10	0	0	0	0.5
9 - 11	0.030742	0.040048	0.040966	1.2
11 - 12	0.030742	0.040048	0.040966	2
11 - 13	0	0	0	2
11 - 14	0	0	0	1.4
14 - 15	0	0	0	1.4
14 - 16	0	0	0	2
16 - 17	0	0	0	2
1 - 18	0.48597	0.068274	0.069839	1.2
18 - 19	0.48597	0.068274	0.069839	0.8
19 - 20	0.48597	0.068274	0.069839	1.6
20 - 21	1.172	0	0	1.4
21 - 22	0	0	0	0.5
21 - 23	1.172	0	0	2
23 - 24	0	0	0	0.5
23 - 25	1.172	0	0	2
25 - 26	1.172	0	0	1.4
26 - 27	1.172	0	0	1
27 - 28	0	0	0	1.4
28 - 29	0	0	0	1.4
29 - 30	0	0	0	2
30 - 31	0	0	0	0.8
29 - 32	0	0	0	2
32 - 33	0	0	0	1.6
33 - 34	0	0	0	0.4
34 - 35	0	0	0	2
32 - 36	0	0	0	0.4
36 - 37	0	0	0	2
37 - 38	0	0	0	1.2
36 - 39	0	0	0	0.5
1 - 40	0	0	0	1.2
40 - 41	0	0	0	0.5
41 - 42	0	0	0	1.4
41 - 43	0	0	0	0.8
43 - 44	0	0	0	0.5
44 - 45	0	0	0	1.6
44 - 46	0	0	0	1
46 - 47	0	0	0	0.5
47 - 48	0	0	0	1.2
48 - 49	0	0	0	1.6
49 - 50	0	0	0	0.5
50 - 51	0	0	0	0.8
49 - 52	0	0	0	1.6
52 - 53	0	0	0	1
53 - 54	0	0	0	1.4
54 - 55	0	0	0	0.4
55 - 56	0	0	0	0.5
53 - 57	0	0	0	1
57 - 58	0	0	0	1.6
58 - 59	0	0	0	1
59 - 60	0	0	0	1.4
60 - 61	0	0	0	1.6
61 - 62	0	0	0	0.5
48 - 63	0	0	0	0.8
1 - 64	0	0.70009	0	1.6
64 - 65	0	0.70009	0	1
65 - 66	0	0.70009	0	2
66 - 67	0	0.70009	0	0.4
67 - 68	0	0	0	0.4
68 - 69	0	0	0	1
69 - 70	0	0	0	0.4
69 - 71	0	0	0	2
71 - 72	0	0	0	0.4
72 - 73	0	0	0	0.4
71 - 74	0	0	0	0.5
74 - 75	0	0	0	0.5
1 - 76	0	0	0	0.5
76 - 77	0	0	0	1
77 - 78	0	0	0	1.2
78 - 79	0	0	0	0.4
79 - 80	0	0	0	1.6
80 - 81	0	0	0	1.2
81 - 82	0	0	0	2
82 - 83	0	0	0	1.6
82 - 84	0	0	0	1
84 - 85	0	0	0	1.2
1 - 86	0	0	0.71614	1.2
86 - 87	0	0	0.71614	1
87 - 88	0	0	0	1
87 - 89	0	0	0.71614	1.4
89 - 90	0	0	0.71614	2
90 - 91	0	0	0.71614	0.4
91 - 92	0	0	0	0.5
92 - 93	0	0	0	0.5
93 - 94	0	0	0	2
94 - 95	0	0	0	1.6
95 - 96	0	0	0	1
96 - 97	0	0	0	2
94 - 98	0	0	0	1
98 - 99	0	0	0	0.8

consequence of the contribution to the fault by the DG at bus 92. Despite the changes in the behaviour and levels of the fault currents, the tripping of the correct relays (26-27), (66-67), and (90-91) is still maintained at equilibrium as evident in Table 4.3. Fig. 4.4 illustrates the evolution of the global cost function due to the iterative strategy revisions. It is clear that the system converges to an equilibrium in finite time as expected.

The proposed algorithm is also tested on the 14-bus network [24] which depicted in Fig. 4.5. The DGs are connected to buses 4, 5, 10, 13, and 14. This is the same configuration of DGs implemented by [9]. The faults occur at 3, 7, and 12 with probabilities of 20%, 35%, and 45% respectively. The available tripping settings that the relays can choose from are as follows: $[0.2, 0.3, 0.4, 0.6, 0.8, 1.0, 1.2, 1.4, 1.6, 2.0, 3.4, 4.0]$. The order of which the DGs start injecting into the DN is as follows: 1) DG at bus 5 is injecting at a 3 MVA capacity; 2) DG at bus 4 is injecting at a 3 MVA capacity; 3) DG at bus 10 is injecting at an 8 MVA capacity; 4) DG at bus 12 is injecting at a 3 MVA capacity; and 5) DG at bus 13 is injecting at a 3 MVA capacity. The fault currents and relay trip sittings obtained for each DG injection are illustrated in Tables 4.4-4.7. The evolution of the cost in the system for each DG injection is demonstrated in Fig. 4.6, Fig. 4.7, Fig. 4.8, Fig. 4.9, and Fig. 4.10 The maximum DG capacities obtained by [9] and the DG capacities used in the implementation of the proposed algorithm are shown in Tables 4.9 and 4.10 respectively. Table 4.9 indicates that a maximum allowable DG capacity of just 13.3743 MVA across the five DGs. Based on the results depicted by figures 4.6 to 4.10, it can be seen that the minimum cost is maintained at greater DG capacities and as such the proposed algorithm works without a having a restriction on the DG capacities unlike [9] which showed a restriction on the DG capacities as demonstrated by table 4.9. Numerically speaking, the proposed algorithm performed as expected with a total of 20 MVA capacity across the five DGs and can perform at a higher DG capacity.

Table 4.3: Case study 3.

Relay	I_F (bus 27)	I_F (bus 67)	I_F (bus 91)	$TripSetting$
1 - 2	0.029134	0.038071	0.040966	0.4
2 - 3	0.029134	0.038071	0.040966	1.6
3 - 4	0.029134	0.038071	0.040966	0.8
4 - 5	0.029134	0.038071	0.040966	0.5
5 - 6	0.029134	0.038071	0.040966	1.4
6 - 7	0.029134	0.038071	0.040966	1.6
7 - 8	0	0	0	1
7 - 9	0.029134	0.038071	0.040966	1.2
9 - 10	0	0	0	1
9 - 11	0.029134	0.038071	0.040966	1.2
11 - 12	0.029134	0.038071	0.040966	1
11 - 13	0	0	0	1.6
11 - 14	0	0	0	2
14 - 15	0	0	0	0.8
14 - 16	0	0	0	1
16 - 17	0	0	0	0.4
1 - 18	0.48903	0.064904	0.069839	1.4
18 - 19	0.48903	0.064904	0.069839	0.5
19 - 20	0.48903	0.064904	0.069839	0.8
20 - 21	1.1732	0	0	1.2
21 - 22	0	0	0	1.6
21 - 23	1.1732	0	0	1.4
23 - 24	0	0	0	1.4
23 - 25	1.1732	0	0	2
25 - 26	1.1732	0	0	1.2
26 - 27	1.1732	0	0	0.4
27 - 28	0	0	0	0.8
28 - 29	0	0	0	1.6
29 - 30	0	0	0	1.2
30 - 31	0	0	0	0.4
29 - 32	0	0	0	1
32 - 33	0	0	0	2
33 - 34	0	0	0	1.6
34 - 35	0	0	0	0.5
32 - 36	0	0	0	1
36 - 37	0	0	0	1
37 - 38	0	0	0	0.8
36 - 39	0	0	0	1
1 - 40	0	0	0	0.8
40 - 41	0	0	0	1.2
41 - 42	0	0	0	0.5
41 - 43	0	0	0	1.2
43 - 44	0	0	0	0.4
44 - 45	0	0	0	1.2
44 - 46	0	0	0	1.4
46 - 47	0	0	0	0.5
47 - 48	0	0	0	0.4
48 - 49	0	0	0	0.5
49 - 50	0	0	0	1.2
50 - 51	0	0	0	2
49 - 52	0	0	0	1.4
52 - 53	0	0	0	1.6
53 - 54	0	0	0	0.5
54 - 55	0	0	0	0.5
55 - 56	0	0	0	1.4
53 - 57	0	0	0	1.4
57 - 58	0	0	0	2
58 - 59	0	0	0	1.6
59 - 60	0	0	0	0.4
60 - 61	0	0	0	1.2
61 - 62	0	0	0	1
48 - 63	0	0	0	1
1 - 64	0	0.70295	0	1.6
64 - 65	0	0.70295	0	2
65 - 66	0	0.70295	0	0.8
66 - 67	0	0.70295	0	0.4
67 - 68	0	0	0	1.6
68 - 69	0	0	0	0.4
69 - 70	0	0	0	0.8
69 - 71	0	0	0	0.8
71 - 72	0	0	0	1.4
72 - 73	0	0	0	0.8
71 - 74	0	0	0	1.4
74 - 75	0	0	0	0.8
1 - 76	0	0	0	1
76 - 77	0	0	0	0.4
77 - 78	0	0	0	1.4
78 - 79	0	0	0	1
79 - 80	0	0	0	1.4
80 - 81	0	0	0	1
81 - 82	0	0	0	1.2
82 - 83	0	0	0	0.4
82 - 84	0	0	0	1
84 - 85	0	0	0	1.4
1 - 86	0.029798	0.038939	0.71614	1.6
86 - 87	0.029798	0.038939	0.71614	0.8
87 - 88	0	0	0	0.5
87 - 89	0.029798	0.038939	0.71614	1.6
89 - 90	0.029798	0.038939	0.71614	2
90 - 91	0.029798	0.038939	0.71614	0.5
91 - 92	0.029798	0.038939	1.0879	2
92 - 93	0	0	0	0.8
93 - 94	0	0	0	1
94 - 95	0	0	0	2
95 - 96	0	0	0	2
96 - 97	0	0	0	1
94 - 98	0	0	0	0.4
98 - 99	0	0	0	2

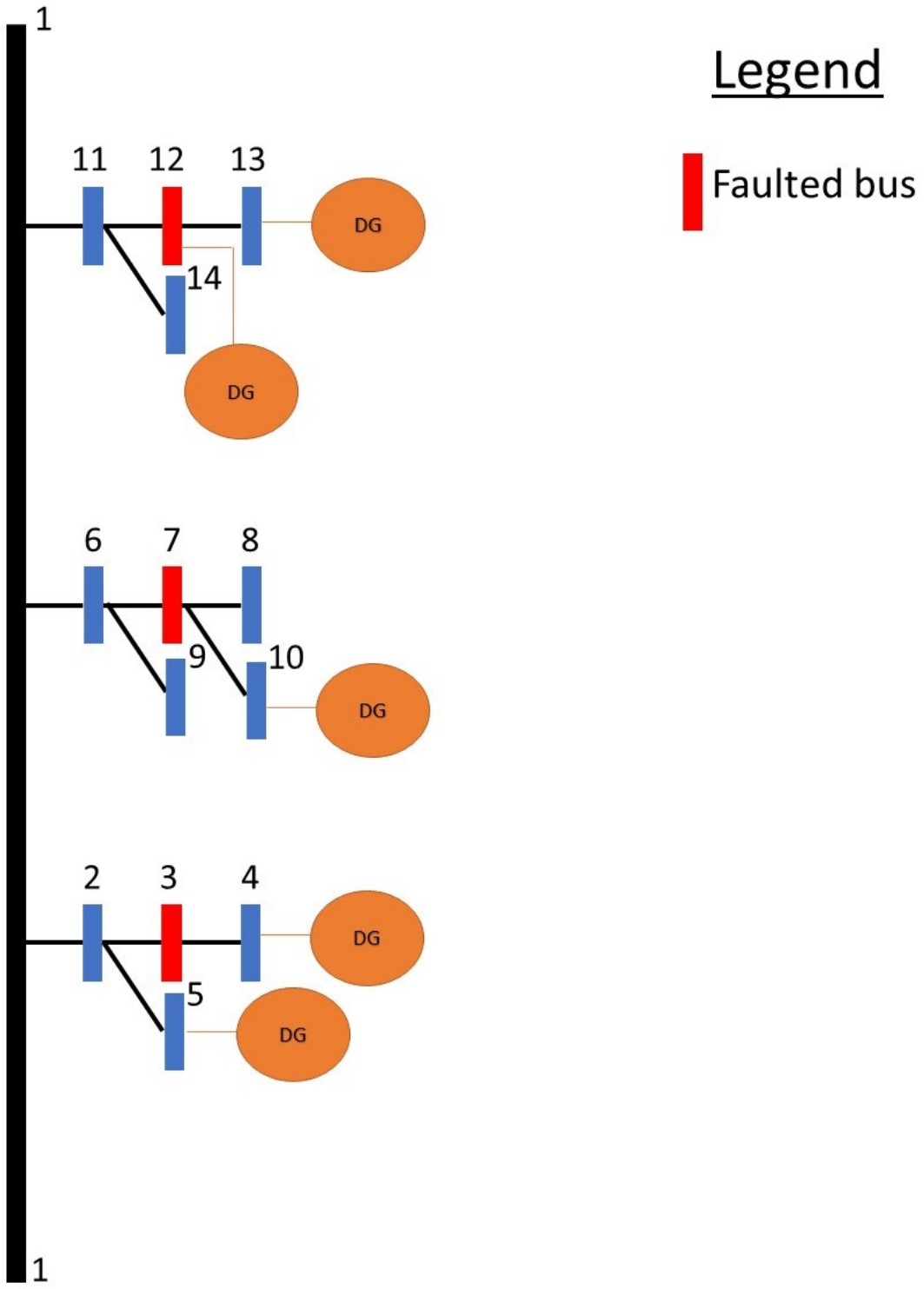

Figure 4.5: 14-bus system.

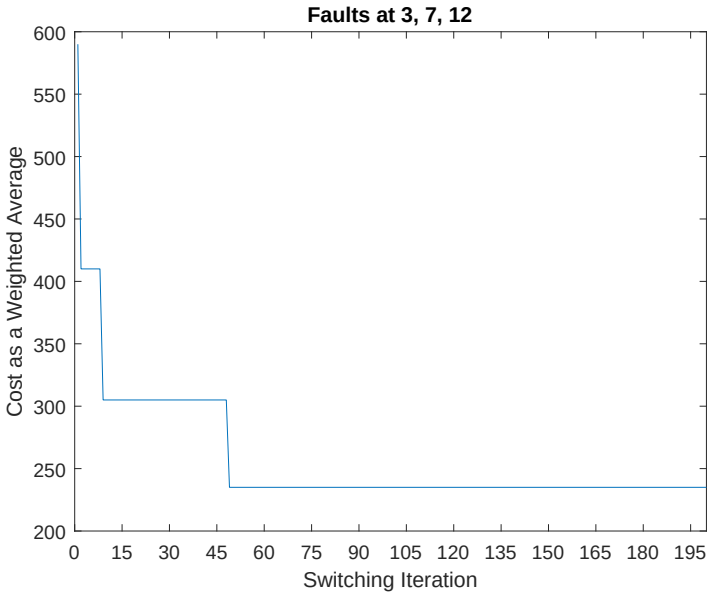

Figure 4.6: Injection by DG at bus 5 begins.

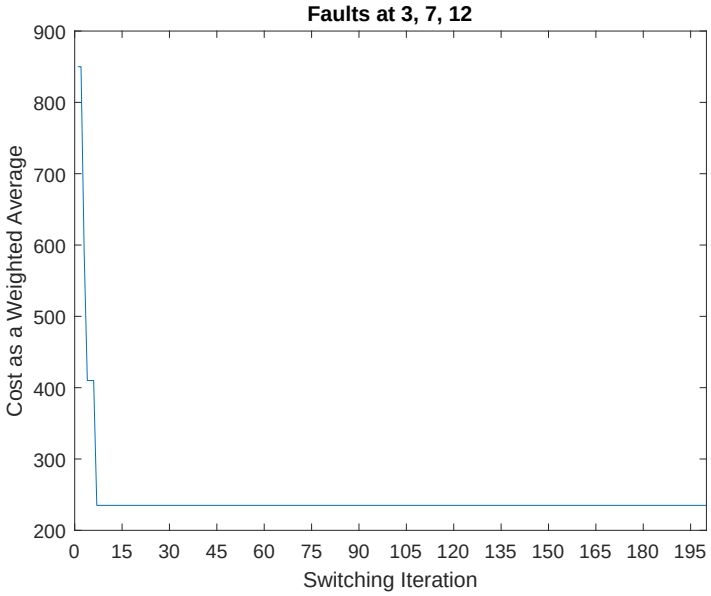

Figure 4.7: Injection by DG at bus 4 begins.

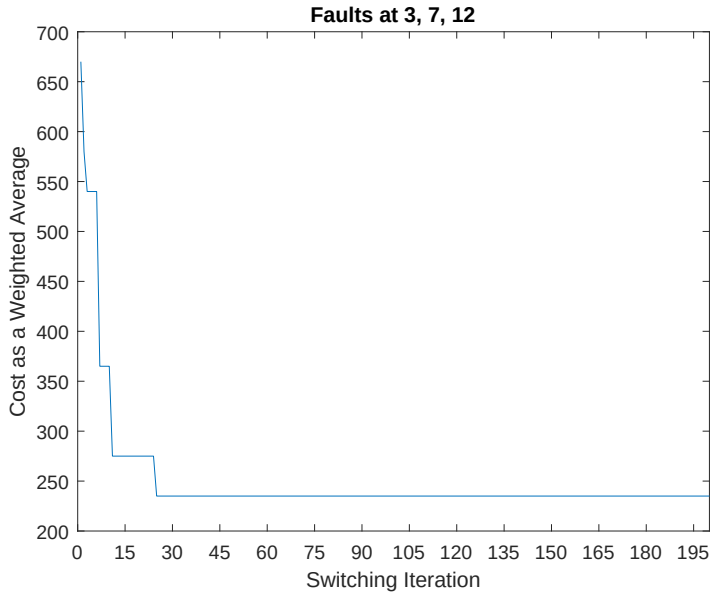

Figure 4.8: Injection by DG at bus 10 begins.

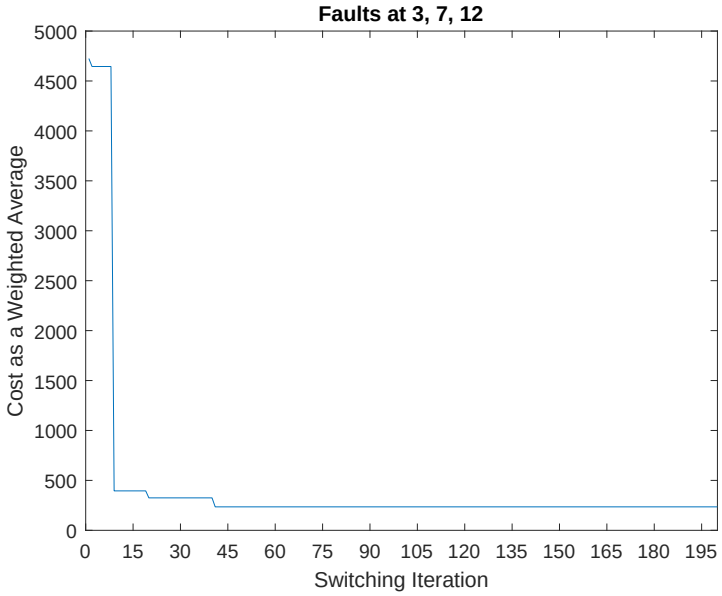

Figure 4.9: Injection by DG at bus 12 begins.

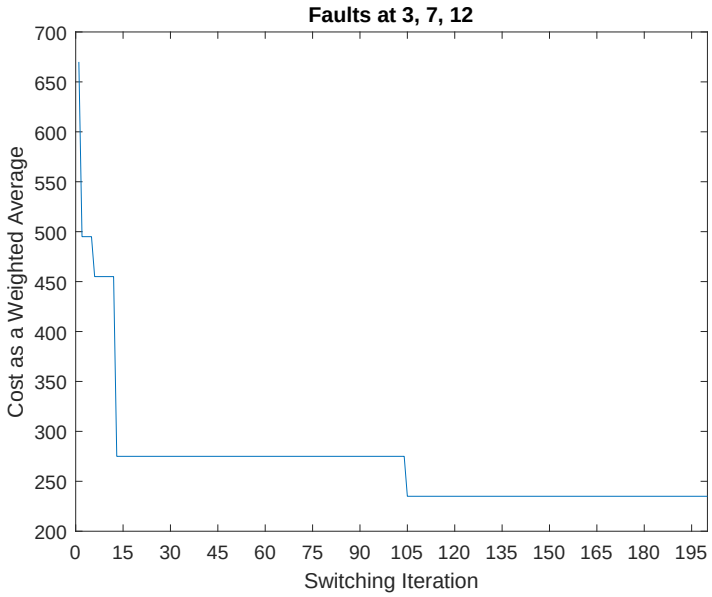

Figure 4.10: Injection by DG at bus 13 begins.

Table 4.4: Injection by DG at bus 5 begins.

Relay	I_F (bus 3)	I_F (bus 7)	I_F (bus 12)	$TripSetting$
1 - 2	1.8872	0.074913	0.074913	2
2 - 3	1.9897	0	0	1.2
3 - 4	0	0	0	3.4
2 - 5	0.070952	0.050631	0.050631	1.6
1 - 6	0	2.6724	0	4
6 - 7	0	2.1473	0	0.2
7 - 8	0	0	0	4
6 - 9	0	0	0	0.6
7 - 10	0	0	0	0.3
1 - 11	0	0	2.6724	4
11 - 12	0	0	2.1473	0.4
12 - 13	0	0	0	0.4
11 - 14	0	0	0	0.2

Table 4.5: Injection by DG at bus 4 begins.

Relay	I_F (bus 3)	I_F (bus 7)	I_F (bus 12)	$TripSetting$
1 - 2	1.8872	0.14303	0.21287	4
2 - 3	1.9897	0.070837	0.068102	0.2
3 - 4	0.17523	0.070837	0.068102	0.3
2 - 5	0.070952	0.048795	0.097843	0.2
1 - 6	0	2.7062	0	4
6 - 7	0	2.1745	0	1.2
7 - 8	0	0	0	0.2
6 - 9	0	0	0	1.2
7 - 10	0	0	0	4
1 - 11	0	0	2.7407	4
11 - 12	0	0	2.2022	1.4
12 - 13	0	0	0	0.2
11 - 14	0	0	0	1.2

Table 4.6: Injection by DG at bus 10 begins.

Relay	I_F (bus 3)	I_F (bus 7)	I_F (bus 12)	$TripSetting$
1 - 2	1.9449	0.14303	0.27191	4
2 - 3	2.045	0.070837	0.13027	0.2
3 - 4	0.17523	0.070837	0.13027	0.8
2 - 5	0.069537	0.048795	0.095742	2
1 - 6	0.19162	2.7062	0.19851	4
6 - 7	0.15397	2.1745	0.15951	1
7 - 8	0	0	0	2
6 - 9	0	0	0	3.4
7 - 10	0.1761	0.51112	0.18244	1.6
1 - 11	0	0	2.8455	4
11 - 12	0	0	2.2864	1
12 - 13	0	0	0	1
11 - 14	0	0	0	0.2

Table 4.7: Injection by DG at bus 12 begins.

Relay	I_F (bus 3)	I_F (bus 7)	I_F (bus 12)	$TripSetting$
1 - 2	1.968	0.13589	0.26901	2
2 - 3	2.0651	0.067438	0.12874	1.6
3 - 4	0.17346	0.067438	0.12874	0.4
2 - 5	0.06764	0.046263	0.094817	0.2
1 - 6	0.18331	2.7389	0.36303	4
6 - 7	0.1473	2.2008	0.29171	1
7 - 8	0	0	0	0.2
6 - 9	0	0	0	0.4
7 - 10	0.16847	0.50653	0.33363	2
1 - 11	0.078946	0.089492	2.9023	4
11 - 12	0.063436	0.07191	2.3321	0.2
12 - 13	0	0	0	4
11 - 14	0	0	0	1.6

Table 4.8: Injection by DG at bus 13 begins.

Relay	I_F (bus 3)	I_F (bus 7)	I_F (bus 12)	$TripSetting$
1 - 2	1.9883	0.13351	0.27868	4
2 - 3	2.0846	0.066254	0.13323	2
3 - 4	0.17357	0.066254	0.13323	0.2
2 - 5	0.06723	0.045456	0.098323	1.2
1 - 6	0.18003	2.7687	0.37469	4
6 - 7	0.14466	2.2247	0.30107	0.6
7 - 8	0	0	0	2
6 - 9	0	0	0	1.4
7 - 10	0.16546	0.50685	0.34434	0.6
1 - 11	0.14886	0.16878	2.9136	3.4
11 - 12	0.11962	0.13562	2.3412	0.8
12 - 13	0.059495	0.067456	0.17523	3.4
11 - 14	0	0	0	0.6

Table 4.9: Maximum DG capacities obtained by [9].

Bus	MVA
5	1.989
4	1.9069
10	6
12	1.7075
13	1.7709

Table 4.10: DG capacities implemented by the proposed algorithm.

Bus	MVA
5	3
4	3
10	8
12	3
13	3

Chapter 5

Conclusion and Future Work

5.1 Conclusion

In this thesis, the proposed decentralized algorithm allows relays to adaptively reconfigure local tripping settings to accommodate changes in the generation capacities of DGs and various faults that can occur in the DN. This adaptive reconfiguration allows for the plug-and-play integration of DGs with varying generation capacities at various points of the DN in a flexible manner. This will pave the path to increasing sustainability and resilience in the changing landscape of the modern DN. The efficacy of the proposed algorithm was demonstrated via comprehensive theoretical and practical studies.

5.2 Future Work

As future works, the theoretical constructs using potential games can be extended to the utilization of population games that can include a larger number of players and most importantly, guarantee convergence to global optima. Additionally, the work can be extended to consider unsymmetrical faults such as line-to-ground faults double line-to-ground faults among other faults.

Bibliography

[1] S. H. Horowitz and A. G. Phadke, *Power System Relaying*. Chichester: Wiley, 2015.

[2] V. Telukunta, J. Pradhan, A. Agrawal, M. Singh and S. G. Srivani, "Protection challenges under bulk penetration of renewable energy resources in power systems: A review," in *CSEE Journal of Power and Energy Systems*, vol. 3, no. 4, pp. 365-379, Dec. 2017, doi: 10.17775/CSEEJPES.2017.00030.

[3] J. Ma, X. Wang, Y. G. Zhang, Q. X. Yang, and A. G. Phadke, A novel adaptive current protection scheme for distribution systems with distributed generation, *International Journal of Electrical Power & Energy Systems*, vol. 43, no. 1, pp. 14601466, Dec. 2012.

[4] M. Ojaghi, Z. Sudi, and J. Faiz, Implementation of full adaptive technique to optimal coordination of overcurrent relays, *IEEE Transactionson Power Delivery*, vol. 28, no. 1, pp. 235244, Jan. 2013.

[5] S. F. Shen, D. Lin, H. F. Wang, P. J. Hu, K. Jiang, D. Y. Lin, and B. T. He, An adaptive protection scheme for distribution systems with DGs based on optimized thevenin equivalent parameters estimation, *IEEE Transactions on Power Delivery*, vol. 32, no. 1, pp. 411419, Feb. 2017

[6] P. H. Shah and B. R. Bhalja, New adaptive digital relaying scheme to tackle recloser-fuse miscoordination during distributed generation interconnections, *IET Generation, Transmission & Distribution*, vol. 8, no. 4, pp. 682688, Apr. 2014.

[7] F. Coffele, C. Booth, and A. Dysko, An adaptive overcurrent protection scheme for distribution networks, *IEEE Transactions on Power Delivery*, vol. 30, no. 2, pp. 561568, Apr. 2015.

[8] P. Mahat, Z. Chen, B. Bak-Jensen, and C. L. Bak, A simple adaptive overcurrent protection of distribution systems with distributed genera-tion,*IEEE Trans. Smart Grid.*,vol.2,no.3,pp.428437,Sep.2011. control strategy for multi-der microgrids-part 1: Fundamental concepts,"*IEEE Trans. on Pow. Del.*, vol. 27, no. 4, pp. 1843-1853, 2012.

[9] H. Zhan et al., "Relay Protection Coordination Integrated Optimal Placement and Sizing of Distributed Generation Sources in Distribution Networks," in *IEEE Transactions on Smart Grid*, vol. 7, no. 1, pp. 55-65, Jan. 2016, doi: 10.1109/TSG.2015.2420667.

[10] J. Chen, R. Fan, X. Duan, J. Cao, "Penetration level optimization for DG considering reliable action of relay protection device constrains," International Conference on Sustainable Power Generation and Supply (SUPERGEN '09), 2009, pp.1-5, Apr. 2009.

[11] M. Singh et al., "Optimal location, size and protection coordination of distributed generation in distribution network," 2013 IEEE Symposium on Swarm Intelligence (SIS), pp.221-227, Apr. 2013.

[12] H. Farhangi, "The path of the smart grid," IEEE Power and Energy Magazine, vol. 8, no. 1, pp. 18-28, 2010.

[13] J. D. Glover, M. S. Sarma, and T. J. Overbye, *Power systems analysis and design.* Thomson, 2007.

[14] Saadat, H., 2010. *Power System Analysis*. [United States]: PSA Pub.

[15] E. Baran and F. F. Wu, Network reconfiguration in distribution systems for loss reduction and load balancing, *IEEE Trans. Power Del.*, vol. 4 no. 2, pp. 14011497, Apr. 1989.

[16] Dov Monderer and Lloyd S. Shapley. Potential games. *Journal of Economic Literature*, 14(44):124143, 1996.

[17] J.R.S.Mantovani,F.Casari,and R.A.Romero,"Reconfigurao de sistemasde distribuio radiais utilizando o critrio de queda de tenso, Revista Controlee Automao," *SBA Controle & Automacao*, vol. 11, no. 3, pp. 150-159,2000.

[18] W. J. Park, B. C. Sung, K. B. Song, and J. W. Park, Parameter optimization of SFCL with wind-turbine generation system based on its protective coordination, *IEEE Transactions on Applied Superconductivity*, vol. 21, no. 3, pp. 21532156, Jun. 2011.

[19]] V. R. Pandi, H. H. Zeineldin, and W. D. Xiao, Determining optimal location and size of distributed generation resources considering harmonic and protection coordination limits, *IEEE Transactions on Power Systems*, vol. 28, no. 2, pp. 12451254, May 2013.

[20] A. Srivastava, J. M. Tripathi, R. Krishan and S. K. Parida, "Optimal Coordination of Overcurrent Relays Using Gravitational Search Algorithm With DG Penetration," in *IEEE Transactions on Industry Applications*, vol. 54, no. 2, pp. 1155-1165, March-April 2018, doi: 10.1109/TIA.2017.2773018.

[21] K. A. Saleh, H. H. Zeineldin, A. Al-Hinai, and E. F. El-Saadany, Optimal coordination of directional overcurrent relays using a new time currentvoltage characteristic, *IEEE Trans. Power Del.*, vol. 30, no. 2, pp. 537544, Apr. 2015

[22] A. A. Balyith, H. M. Sharaf, M. Shaaban, and E. F. El-Saadany, and H.H. Zeineldin, Non communication-based time-current-voltage dual setting directional overcurrent protection for radial distribution systems with DG, *IEEE Access*, vol. 8, pp.190572190581, 2020.

[23]] M. Lwin, J. Guo, N. B. Dimitrov, and S. Santoso, Stochastic optimization for discrete overcurrent relay tripping characteristics and coordination, *IEEE Trans. Smart Grid*, vol. 10, no. 1, pp. 732740, Jan. 2019.

[24] S. Civanlar, J. J. Grainger, H. Yin, and S. S. H. Lee, Distribution feeder reconfiguration for loss reduction, *IEEE Trans. Power Del.*, vol. 3, no. 3, pp. 12171223, Jul. 1988.